Towards an Integrated Observing Platform for the Terrestrial Water Cycle:

From Bedrock to Boundary Layer

By

Christopher Duffy (SSG, chair), Roni Avaissar, Cliff Dahm, Ken Davis, Michael Dettinger , Jim Hack , Danny Marks, Mark A. Miller, Roger Pulwarty, Marty Ralph, Maurice Roos, Christina Tague

Science Steering Group (SSG) of the Interagency Working Group (IWG)
of the
Climate Change Science Program (CCSP)
Global Water Cycle Research Element

Towards an Integrated Observing Platform for the Terrestrial Water Cycle:
From Bedrock to Boundary Layer

Introduction

The "State" of Water Cycle Science

The circulation and exchange of water and energy across the shared boundaries of the atmosphere, continents and oceans defines the global water cycle. Conceptually, these fluxes determine the "state" of the earth-climate system, however the domain, function and linkages of significant components of this system are poorly understood, and either unmeasured or only partially measured. In this paper, the Science Steering Group for the CCSP Water Cycle Research Program proposes a fundamentally new design for an integrated water cycle observing platform that will revolutionize our "way of seeing" the hydrologic cycle. To be successful the concept will require detailed coordination and broad participation across the Water Cycle research community. Furthermore, given the importance of seasonal and longer time scales and trends to the intensity of hydroloclimatic events, this effort will need coordination of short-term campaign-style IOP's (Intensive Operation Period), and placed-based, fixed-sensor, long-term monitoring typical of watershed investigations. In this paper we explore this new arena of integrated measurements as a mechanism for interdisciplinary science and as a bridge to understanding interfacial fluxes across these boundaries.

Fact: *Our inability to close the water/energy balances at the river- basin scale crystallizes the scientific gap in our understanding of the terrestrial components of the water cycle. Models, have reached an "information limit" (ref..) with poorly resolved and unmeasured processes and parameters.*

The last few decades have seen major advances in water cycle research. Nonetheless, the pace of scientific achievement in water cycle research is slowing, largely due to the discovery that the atmosphere, ecology, ocean margin, and terrestrial hydrology are more strongly coupled than previously thought, and traditional measurement strategies have been insufficient to quantify these relationships. Integrated understanding is essential to closing water and energy budgets at the natural scales of this complex system. While models have been very useful, their value also is limited due to strong scale dependencies, artificial boundaries, and poorly resolved processes. In order to address this "closure" problem, new experiments and advanced observing systems, fully integrated with theory, must be designed. A new generation of observations must recognize the natural landscape boundaries and scales where the atmosphere, vegetation and subsurface partitions interact. The intersection of the terrestrial scales associated with hillslopes, watersheds, and river basins, with ecological regions, estuaries, subsurface linkages, and meso-scale weather must be the foci for a more coherent system of observations. The goal of this paper is to propose an initial experiment to advance the problem of closing water, energy and solute budgets more appropriately, and to promote a deeper understanding of the fundamental coupled processes and feedbacks that will lead to improved predictive capability of the terrestrial water cycle.

Improvements in the prediction of water cycle phenomena will require process-level understanding, supported by innovative instrumentation, and comprehensive observational networks. The experimental design supports research regarding feedbacks and coupling of atmosphere, land and subsurface processes, including integration with long term coordinated data sets and model products (NCEP, 2005). As an example, it is

known that clouds and precipitation strongly affect both the atmosphere and terrestrial systems and serve as primary avenues for their interactions. However, boundary layer research has not traditionally looked at seasonal or longer-term changes in evaporation and transpiration resulting from dynamic soil moisture below the root zone including the shallow water table. Likewise, the impact of complex terrain on regional moisture and energy balances may play important roles in soil moisture redistribution and longer-term memory of the watershed function.

Although important research is underway, an observing system with simultaneous measurement of all major components of the water cycle, including atmospheric processes, the terrestrial hydrologic fluxes related to soil moisture and water table states, and vegetation dynamics, has not yet been attempted. The question we pose here is: *What would such an observing platform look like?*

In this paper we focus on elements of design for a new observing strategy for the continental component of the water cycle. In particular we propose an instrument platform that emphasizes sensor integration and coordination of data streams within the natural space and time scales of the terrestrial water cycle. We use the watershed as the organizing principal at the regional scale, and the physical properties of the watershed as the basis for sensor deployment. At the local scale, sensor systems are deployed within a vertical and horizontal domain, which extends from the base of active groundwater circulation, through the soil, vegetation and the top of the atmospheric boundary layer. The flexible design must be able to take advantage of the natural scales of motion for water, energy, and should be adaptable to most physiographic and climatic settings.

A regional hydroclimatic framework defined by the watershed or river basin, will necessarily represent coupled processes and feedback loops operating over a wide range of time scales including: boundary-layer dynamics, vegetation growth, soil moisture, groundwater level changes, and stream runoff response. At present there is no observing system that takes advantage of coordinated measurements at the local-to-regional scale. Clearly, this would require substantial multi-disciplinary coordination for design and implementation. However, such a system would be a model for scientific cooperation in support of a national observing system, while at the same time recognizing the unique needs and mission of each federal agency involved in the environmental observations.

Basic Requirements of an Observing Platform

The National Research Council report, “Basic Research Opportunities in the Earth Science,” outlines the need for “integrative studies in the critical zone” (NRC 2001). The critical zone is identified as, "the heterogeneous near-surface environment in which complex interactions of rock, soil, water, air and living organisms regulate the natural habitat and determine the availability of life-sustaining resources.” Given the motive of integrative research by scientists and science funding agencies, a first step is to re-examine our approach to scientific observing systems, and search for coherence among existing capabilities of ground-based and coordinated satellite or aircraft observations. The observation network deployed for a particular research experiment or campaign carried out within the “critical zone”, must be designed such that all relevant fluxes or states observed by the sensor system are measured simultaneously. It should have as its central motivation, an improved predictive capability of integrated atmosphere-terrestrial dynamics at relevant human and/or ecological time scales. Ultimately it should provide the experimental and theoretical evidence necessary to evaluate the function and security of the nations water supply and serve as a framework for integrated decision-making under conditions of secular change, extreme events and long-term variability. At the outset, the initial scientific experiment should help to develop an optimal strategy for identifying the needs for in-situ observations in support of water cycle science and agency goals/mission. The observing platform should be deployed to complement and extend the national observing system (e.g. NOAA, NASA, USGS, USDA, DOE, EPA, etc.) presently deployed.

An important criterion for a new scientific observing system is the ability to detect and attribute change. To what degree our ability to evaluate change has been limited by our observing system is unknown at present. One goal of this paper is to propose a design for an observing platform where all important fluxes in some limited domain are observed coherently. Toward this end we have proposed here a definition of the "critical zone" of the terrestrial water cycle as a volume bounded in areal extent by the watershed, bounded vertically by the depth of active groundwater flow below, and by the depth of the atmospheric boundary layer above. We note that at the upper and lower limits of this domain, there is still exchange of energy, mass, and momentum, and that explicit conditions will be necessary for entrainment and exchange with regional atmosphere and regional groundwater circulation.

A platform for observing the water cycle within the "active zone" will require:

- integrated sensors be deployed within and over the watershed control volume and sampled such that a complete picture of the atmosphere-land-surface-vegetation-subsurface couplings and feedbacks be identified, physically represented, and implemented in a new class of fully coupled models.
- a data management strategy should be implemented, and maintained from the outset with standardized sensor interface protocols.
- the initial experimental sites should be chosen to maximize the prospect of early success (e.g. extensive historical experimental and operation data and site information available).
- continuous, real-time observations at time scales of seconds to decades
- spatial measurements across scales from sub-meter to 10's of kilometers
- continuous operation with two-way transmission of data and sensor control with adaptive sampling during extreme events
- facilities for instrument maintenance and calibration.

A Parsimonious Conceptual Model

The Regional Scale

Knowledge follows systematic observation. The present "observation gap" in the terrestrial hydrologic cycle cannot be resolved unless all the components of this system are simultaneously observed at characteristic locations, at appropriate scales and within the operating resolution and range of current instrumentation. As a first step towards resolving this observation gap, we discuss the physical domain within which integrated observations are feasible to resolve the scales of motion over which feedbacks and fluxes are relevant to human and other terrestrial life, and where improvements in predictive skill are currently deemed necessary. The goal is to establish quantitative relationships among all fluxes affecting the water cycle over time scales of events (minutes to days), diurnal, to seasonal, interannual, and eventually to decadal time scales; and to develop an observing system that can begin to resolve the interface-physics of the atmosphere, biosphere, and regolith or subsurface domain. This effort should initially be carried out at field stations or experimental basins/watersheds which have a significant historical data set, and at sites with significant geophysical and biological relevance (e.g. characteristic climate zone, terrain, vegetation, hydrogeology, land use, etc.). The initial domain of the experiment will be crucial to scientific success and long-term support. An experiment to study the water cycle variability over this range of time scales will require both a focus on processes within the region of interest, as well as the linkages with water sources and climatic forcing from the surrounding region. The proposed spatial domain is defined by the intersection of the natural boundaries that organize flows of water and energy within the terrestrial water cycle, watershed and the atmosphere. The relevant projection on the

earth's surface is taken to be the watershed (micro-mesoscale: <1-100 km), which identifies an important and unresolved length-scale of fluid motion on the continents, and reflects the local evolution of continental tectonics, chemical weathering, soil formation, erosion, and sedimentation histories. Figure 1 (ref. NASA) illustrates the necessary local to regional and global spatial scales and the implicit time scales of the water cycle.

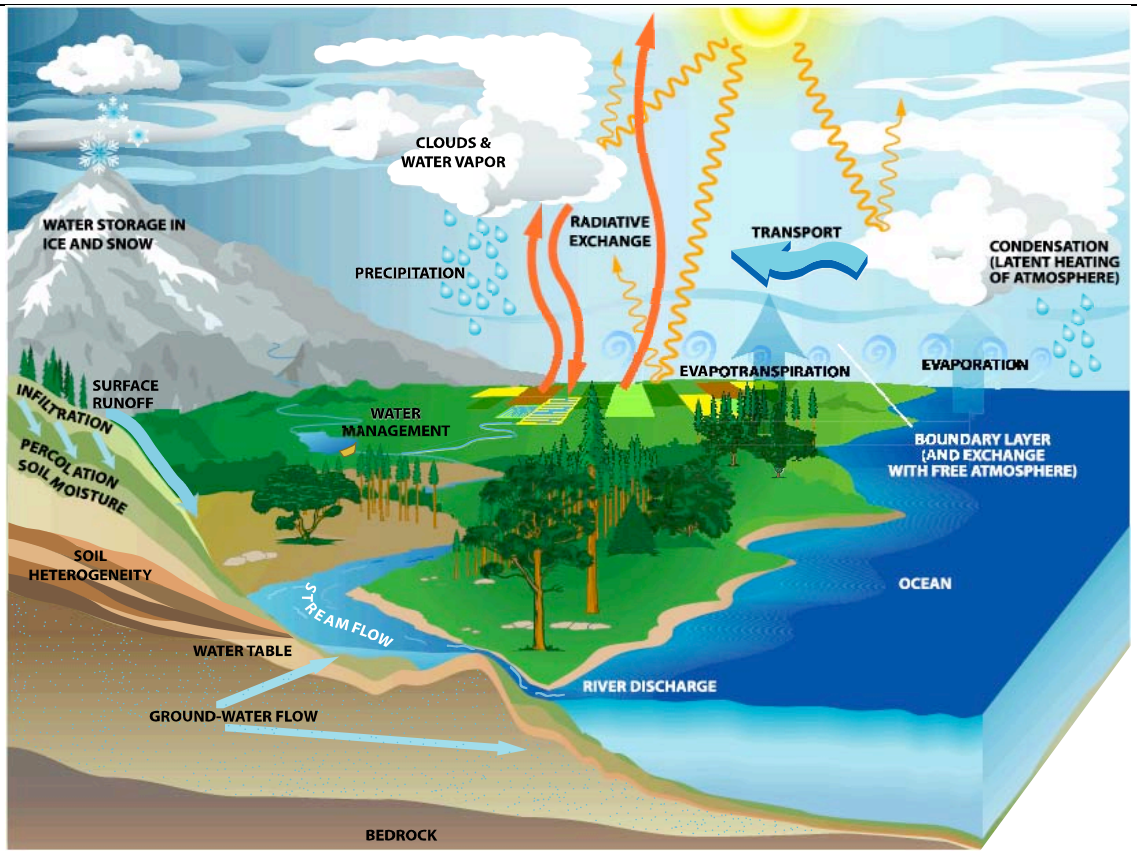

Figure 1. The hydrologic cycle and the broadly defined processes contributing to circulation of water and energy (NASA)..

For the purposes of this paper, it is necessary to be more explicit about the domain of a water cycle observing platform proposed here. From the land surface, we project the watershed boundaries vertically downward to include an effective depth of active susbsurface flow, and upward through the soil, root zone, canopy, to the top of the well-

mixed atmospheric boundary layer. The conceptual domain is illustrated for the Little Washita River Basin in central Oklahoma in Figure 2. The effective depth of active flow is conveniently defined as a limited region below the land-surface where soil moisture and groundwater are influenced by time scales of local weather and climate, and we refer to this zone as the subsurface boundary layer (*SBL*). A more precise definition of the *SBL* is that the *SBL* is the depth which feels the effect of the local atmosphere within the areal footprint of the watershed. From a practical point of view, the water table carries much of the subsurface information below the root zone, serves as the lower boundary condition for soil moisture, and represents the potential surface that forces the translation of water to streams and rivers. The *SBL* is located within the regolith, or the uppermost layer of the lithosphere that has been formed by mass movement, weathering, erosion, or deposition of unconsolidated or consolidated material. It includes the soil, biomass, fractured and weathered bedrock, alluvium, colluvium, and actively flowing groundwater. Note that the *SBL* may still exchange mass with deeper subsurface layers, but the latter are not strongly affected by surface atmospheric conditions within the watershed.

We take the upper limit of the control volume to be the variable height of the atmospheric boundary layer (*ABL*). This layer is most strongly influenced by local surface fluxes and, less directly so, by conditions in the overlying (non turbulent) “free” atmosphere. For the purpose of water and energy cycle investigations, the *ABL* is typically on the order of 1 km thick during daylight hours when the surface is warm, collapsing to order of 100 m thick during nighttime hours or when the surface is colder than the ABL. The top of the ABL, and thus of the proposed control volume, is generally

marked by a temperature inversion that serves to largely cap the rise of *ABL* turbulence and mixing, and thus to separate the *ABL* (and surface) from the overlying free atmosphere, which typically participates more strongly and directly in the large-scale, climate-scale atmospheric circulations than does the surface-coupled *ABL*.

The *ABL* closely reflects, responds to, and determines the rates of, surface heat and moisture fluxes. The thickness and properties of the *ABL* are continually evolving in a complex accommodation of changes in both surface- and free atmospheric conditions. The *ABL* grows by turbulent entrainment of warmer and usually drier air from the overlying free atmosphere in response, usually, to the same surface processes that help to establish near-surface temperatures and humidities. Thus the evolution of the ABL, which passes through regular daily and seasonal cycles, is capable of continually feeding back onto surface processes, including ET rates, in ways that are not generally incorporated into hydrologic models or observations to date (Margulis and Entekhabbe, 2004).

The transition layer in this conceptual model, necessarily intersects the *ABL* and the *SBL,* as this zone encompasses intercepted water in above ground vegetation, litter, rooting depth, as well as surface detention storage as either snow or standing surface water and subsurface frost.

Each process layer of the experiment (subsurface, root zone-canopy transition and atmospheric boundary layer) is an explicit physical system where governing transport equations can be applied. The observing platform, should support fundamental research into understanding and quantifying the physical processes, coupling, and feedback across these layers, including testing of new algorithms and modeling systems. Some of the

relevant processes include: the transport of water and energy across the atmosphere-land surface interface; the relation of water, carbon, nitrogen, and vegetation; the formation and dissipation of clouds; the interactions of cloud microphysics and atmospheric mixing processes; the mechanisms determining precipitation and precipitation efficiency; the rates and distribution of groundwater recharge; and the groundwater-stream relationship.

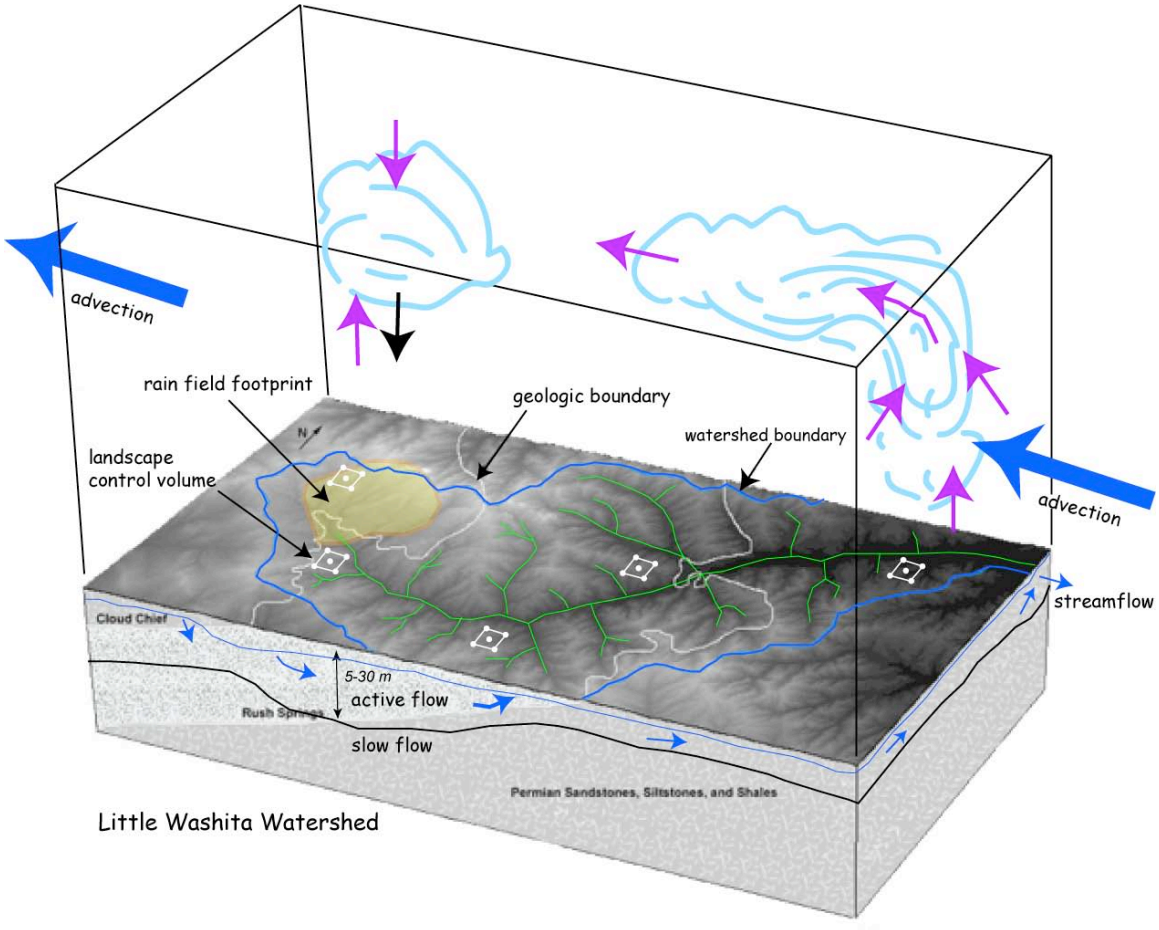

Fig 2. The regional conceptual model defined by the atmospheric boundary layer (ABL) including a limited subsurface region below the land-surface where the water table influences both soil moisture and groundwater flow over time scales important to local weather and climate (subsurface boundary layer, SBL). This domain serves as a hydrologic framework for defining a coherent system of observations strategically deployed to observe water and energy budgets at the natural space and time scales operating within the watershed.

The time scales of near-surface boundary-layer turbulent (eddy) transport represents the shortest time scales of the experiment, and the relation of turbulent transport of mass and momentum to canopy moisture state must be resolved through new and coordinated instrumentation. The shallow water table and lateral groundwater flow represent the longest time scales of the experiment. The water table serves as a measure of the fluid potential controlling the supply of water to streams (baseflow), and also serves as a lower boundary condition to soil moisture fluxes (e.g. recharge, infiltration and evapotranspiration). Although groundwater exists at greater depths, in this experiment our concern is the active flow-depth through which water circulates at relevant time scales for the watershed (e.g. storm event, diurnal, seasonal, interannual, and decadal). Between the time scales of turbulent surface fluxes and groundwater flows, storm scale processes, such as infiltration, saturation, inundation, and runoff, and diurnal time scales, which dominate the daily growth-collapse cycles of ABL properties, establish two other key time scales that can be tracked by the integrated observing platform.

Over larger scales, when fluxes of mass, energy, and momentum enter or leave through lateral boundaries of the experimental domain, the corresponding flux at each level of the control volume should be thought of as a boundary flux interacting with a larger scale motion. Exchanges of mass, energy and momentum between process layers in the control volume, represent both forcing and feedback in the system. In any investigation of the complex earth system where one attempts to measure the time scales of change of a phenomenon or a limited range of phenomena, it is always the case that hidden or unobserved variables are present. One practical goal of this experimental

design is to isolate the essential state variables of the limited system and to prioritize or eliminate secondary variables in the physical formulation.

Critical components of the observing system then will be design features and observations that characterize the interfacial fluxes within the control volume as well as the fluxes on the external surface of the control volume. A focus on watershed scale control volumes ensures that surface fluxes of water and heat (at least) do not cross the lateral boundaries at the surface in more than a few well contrained points. An initial focus on watersheds that also are closed in the SBL also simplifies observation and analysis. Transport into and out of the lateral boundaries of the control volume through the ABL, and changes in the overlying free atmosphere, will necessarily be estimated or observed. Consequently the atmospheric fluxes of heat, momentum, and water vapor at the edges of the control volume will need to be characterized with a combination of byproducts from large-scale data assimilation or atmospheric models and by two or more atmospheric profilers of ABL thickness, winds, temperatures, and vapor operating near the edges of the study areas for at least the intensive observation periods. These products and observations have not been included in past hydrologic observatories, but will play a key role in characterizing the ABL conditions above the vegetation and land surface layers.

The Local or Landscape Scale

The surface exchange and transport of water and energy within the watershed domain described above, represents a unique challenge to integrated water cycle research. To this point we have attempted to make the case that the major roadblock to

understanding the water cycle at this scale is the lack of coordinated or coherent measurements at the natural scales of the terrestrial water cycle. There should be no illusions about the scope of this effort. It is a significant scientific and institutional challenge. The present limited experiment would require coordinated observations of the atmosphere (e.g. water vapor, winds, thermodynamics, cloud-radiative forcing, and precipitation), the near-surface (e.g. surface exchange fluxes of heat, momentum and moisture, including transpiration, along with radiation balances, vegetation dynamics, precipitation, and runoff), and the subsurface (e.g. soil moisture, temperature, pressure profiles, water table and baseflow). The control volume itself will require geophysical and biophysical characterization. It is expected that any site chosen should have a completed (or anticipated) digital watershed survey available for soils, geology, vegetation, high resolution topography, in addition to the hydroclimatic database. To be truly useful, the data products generated will require special care in the data acquisition, quality assurance and in the format of the measurements. In particular, the location of the environmental sensors and instrumentation relative to the control volume will require precise placement if a truly useful 4-D data set is to emerge.

The central design criterion for an observing platform of the atmosphere-surface-subsurface is the requirement of coherent physical observations capable of capturing the essential physical processes and feedbacks of mass and energy exchange within a clearly defined system. Figure 3 illustrates the local control volume for the "active zone" divided into three partitions: 1) the atmosphere from land surface to the *ABL*, 2) a transition sub-volume, including the land-surface and near surface processes (canopy, root system, snow, frost, etc.) and, 3) the regolith from land surface to the depth of the *SBL*. Within

each partition, hydrodynamic equations are formed to quantify the states and fluxes within and across the boundaries of the partition, noting that turbulent processes dominate above and non-turbulent below the landsurface. Compatibility in flux across all boundaries is a requirement of the system design.

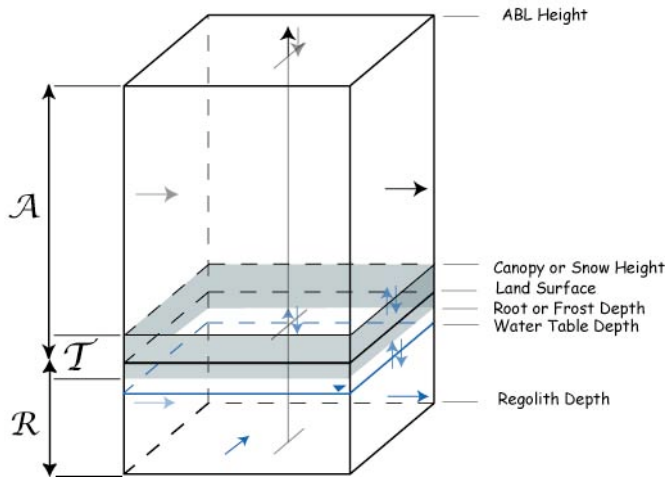

Figure 3. Control volume for local partitioning of moisture and energy fluxes defining surfaces and layers: $\mathcal{A}$-atmosphere, $\mathcal{T}$-transition, $\mathcal{R}$-Regolith. The control volume defines an explicit local domain for the design and deployment of integrated sensors and for which balance equations can be written.

The proposed strategy of integrated measurements allows the application of hydrodynamic theory in the estimation of a detailed balance across the three partitions defined by the control volume as shown in Figure 3. We develop the balance equations next in terms of the partitions which make up the control volume.

Balance Equations for the Control Volume

The atmosphere-biosphere-subsurface exchange of energy and mass is modulated by wide range of feedback processes, all of which need to be resolved for understanding mechanisms, resolving fluxes, and improving the predictability of our physical models. According to Denmead et al (1996), Ek and Holtslag (2004), Margulis and Entekhabbi (2001), Duffy (2004) and others, these local feedback processes may include: 1) radiative feedback from the effect of surface temperature on outgoing longwave radiation, 2) physiological feedback from the interaction of vegetation with surface energy and moisture, 3) aerodynamic feedback, where atmospheric stability and height of the boundary layer affect turbulent heat and moisture exchange and the size of the effective atmospheric reservoir into which surface fluxes mix and equilibrate, 4) convective boundary layer feedback through coupling with surface energy and moisture, conditions in the overlying troposphere, and the direct and indirect effect of clouds, and 5) subsurface feedback where a shallow water table serves as a lower boundary for upward flow of moisture by capillary forces and hydraulic lift by plants, and where infiltration and recharge to a water table introduce a loss to plant available moisture.

An essential step in the experimental design for states and fluxes within the local control volume of Figure 2, is the formulation of approximate balance equations for each layer and the flux exchange across the interfaces between the layers. The purpose of developing approximate balance equations is to demonstrate the most important states/fluxes that must be measured or estimated simultaneously for the proposed experimental platform. It will also be shown how the system of equations is especially important where all terms in the equation cannot be estimated due to measurement

uncertainty or sensor failure in one domain. The atmosphere-transition-regolith exchange of energy and moisture within the control volume of Fig. 3, defines layers and layer heights as a basis for defining average states and fluxes amenable for sensor deployment, data assimilation and flux estimation. Our goal here is not to present a parameterization, but rather to outline the broadly defined physical processes observed within the bedrock to boundary layer control volume. Deployment of an observing system will require further assumptions (e.g multiple soil layers, partitioning of vegetation types, etc.) depending on local conditions and experimental objectives.

Developing the balance equations for the control volume proceeds by integration of prognostic equations describing appropriately averaged states within each layer that are coupled through the boundary fluxes at each interface of the control volume. The column is naturally partitioned into mass balance equations for turbulent exchange within the atmospheric boundary layer ($\mathcal{A}$), non-turbulent transport in the upper-most part of the lithosphere or the regolith ($\mathcal{R}$), and a transition layer ($\mathcal{T}$) that spans both. The general equations for each partition is discussed next.

Atmosphere Control Volume: $\mathcal{A}$

The states (temperature, moisture, and height) of the $\mathcal{A}$ layer evolve in response to surface fluxes of heat, vapor and buoyancy arising from wind stress and surface heating, in response to entrainment of air from the overlying free atmosphere, and in response to advection by near-surface winds. The well-mixed $\mathcal{A}$ layer has a thickness, h, that varies in time and space, from >100 m under stable conditions to ~1 km and more

under unstable conditions. The growth and dissipation of the boundary layer is a critical element of the overall balance and has been treated by several authors (Tennekes, 1973; Smeda, 1979; Margulis and Entekhabi, 2001; Ek and Holtslag, 2004).

The flux form of the conservation equations for energy in the form of potential temperature, and the fluid continuity equation for an arbitrary scalar ξ are:

$$\frac{\partial \overline{\xi}}{\partial t} + \frac{1}{\rho_0}\nabla\bullet\rho_0 V\xi + \frac{1}{\rho_0}\frac{\partial(\rho_0 \overline{w}\overline{\xi})}{\partial z} = -\frac{1}{\rho_0}\frac{\partial F_\xi}{\partial z} + S_\xi \tag{1.1}$$

where $V = \{u, v\}$, and $F_\xi = \rho_0 \overline{w'\xi'}$ represents the vertical turbulent flux of ξ. The separate horizontal and vertical divergence terms in 1.1 are written in terms of a time-average and perturbation (e.g $\xi = \overline{\xi} + \xi'$). S_ξ represents a sources of ξ. The horizontal divergence terms are presented in unperturbed form for simplicity. It is convenient to introduce the conservation of momentum at this point in a similar form as 1.1,

$$\frac{\partial \overline{V}}{\partial t} + \mathrm{V}\nabla\bullet\mathrm{V} + \overline{w}\frac{\partial(\overline{V})}{\partial z} = -\frac{\partial \mathrm{F}_V}{\partial z} + \frac{1}{\rho_0}\nabla\overline{p} + f\ \mathrm{k}\ x\ \overline{V} \tag{1.2}$$

where F_V represents the vertical components of turbulent momentum flux, p is pressure, f is the Coriolis parameter, with the additional assumptions of an incompressible fluid and viscous forces are small.

The next step is vertical averaging of 1.1 over the depth of $\mathcal{A}$. Integrating 1.1 for ξ from a fixed canopy height (z_c) to the top of the boundary layer (z_a) yields:

$$\begin{aligned} &\rho_0 \frac{\partial}{\partial t}\int_{z_c}^{z_a} \overline{\xi}\, dz - (\rho_0\xi)_{z_a}\frac{\partial z_a}{\partial t} + \nabla\bullet\int_{z_c}^{z_a}(\rho_0\xi\mathrm{V})dz - \rho_0(\xi\mathrm{V})_{z_a}\bullet\nabla z_a \\ &+ \rho_0(\xi w)_{z_a} = (F_\xi)_{z_c} - (F_\xi)_{z_a} + \int_{z_c}^{z_a}\overline{S}_\xi dz \end{aligned} \tag{1.3}$$

where the lower boundary z_c is assumed a constant surface allowing turbulent exchange. Following the approach of Lilly (1967) and Randall (2003), equation 1.3 is greatly simplified by defining the vertical turbulent flux as we approach the boundary from below ($z - \varepsilon = z_a$) and from just above the layer ($z + \varepsilon = z_a^+$),

$$\frac{\partial}{\partial t}\int_{z_a}^{z_a^+}\xi dz + \xi_{z_o^+}\frac{\partial z_a^+}{\partial t} - \xi_{z_a}\frac{\partial z_a}{\partial t} + \nabla\bullet\int_{z_a}^{z_a^+}\xi \mathrm{V}\, dz - (\mathrm{V}\xi)_{z_a}\bullet\nabla z_a + (\mathrm{V}\xi)_{z_a^+}\bullet\nabla z_a^+ + (w\xi)_{z_a} - (w\xi)_{z_a^+} = (F_\xi)_{z_a} - (F_\xi)_{z_a^+} + \int_{z_a}^{z_a^+} S_\xi dz \tag{1.4}$$

Letting the integral terms in 1.4 go to zero as $z_a \to z_a^+$, and assuming the turbulent flux above the boundary layer $(F_\xi)_{z_a^+} = 0$, yields a balance

$$\xi_{a^+}\frac{\partial z_{a^+}}{\partial t} + (\mathrm{V}\xi)_{a^+}\bullet\nabla z_{a^+} - (w\xi)_{a^+} = \xi_a\frac{\partial z_a}{\partial t} + (\mathrm{V}\xi)_a\bullet\nabla z_a - (w\xi)_a = (F_\xi)_{z_a} = -\Delta\xi(E - C) \tag{1.5}$$

where $\Delta\xi(E - C)$ is interpreted as the net flux of ξ per unit area across the top of the boundary layer due to turbulent entrainment of air from the free atmosphere.

Substitution of 1.5 into 1.3 and simplifying yields the mass conservation for scalar transport of ξ within $\mathcal{A}$:

$$\rho_0\frac{\partial(\bar{\xi}h)}{\partial t} + \nabla\bullet(\rho_0\xi\mathrm{V}h) - \Delta\xi(\mathrm{E\text{-}C}) = (F_\xi)_{z_c} + \bar{S}_\xi h \tag{1.6}$$

where *h* is as the height of the boundary layer . It is noted that by letting $\xi \to 1$ we have a mass conservation for the total ABL in the form (Randall, 2003):

$$\rho_0\frac{\partial h}{\partial t} + \nabla\bullet(\rho_0\mathrm{V}h) = E - C \tag{1.7}$$

To further simplify the form of the mixed-layer model, we assume hydrostatic conditions, an incompressible fluid, the horizontal divergence terms are small (vertical

turbulent transport), no internal sources or sinks, and replace $\xi \to \{\theta, q\}$. By combining the reduced forms of 1.6 and 1.7, dropping the overbar notation, the balance equations for the specific humidity and the potential temperature have the form:

$$\begin{aligned} \rho_0 h \frac{dq}{dt} &= E_h + E_c - P \\ \rho_0 c_p h \frac{d\theta}{dt} &= (H_h + H_c) + (R_{a+\downarrow} + R_{c\uparrow})\varepsilon - (R_{a\downarrow} + R_{a\uparrow}) \end{aligned} \tag{1.8}$$

where $E_h = \rho_0 \Delta_q \frac{dh}{dt}$ is the entrainment flux for q, $H_h = \rho_0 \Delta_\theta \frac{dh}{dt}$ is the entrainment flux for θ, H_c = the sensible-heat flux from the canopy, E_c = the latent-heat flux from the canopy, $\Delta_q = q_h - q_h^+$ and $\Delta_\theta = \theta_h - \theta_h^+$ measure the jump discontinuity between the ABL states and overlying states in the free atmosphere (Tennekes, 1973; Smeda, 1979; Ek and Holtslag, 2004). In particular, $\Delta\theta$ is the strength of the temperature inversion that caps the *ABL*; the larger the inversion the slower the growth of ABL thickness for a given rate of buoyancy (sensible-heat) flux from the canopy layer. Radiative flux enters the boundary layer from the free atmosphere ($R_{a+\downarrow}$), from the canopy below ($R_{c\uparrow}$) and from the ground ($R_{g\uparrow}$). The emissivity of the boundary layer is ε. Radiative cooling within the boundary layer occurs as upward and downward source terms with fluxes ($R_{a\uparrow}, R_{a\downarrow}$). Figure 4 illustrates the profile for q and θ over the mixed layer in $\mathcal{A}$, and anticipates how this profile interacts with $\mathcal{T}$ and $\mathcal{R}$ which are discussed next.

The momentum equations with the same assumptions (Stull, 1989) have the form

$$\begin{aligned} h \frac{d\overline{u}}{dt} &= (\overline{w'u'})_{z_c} - (\overline{w'u'})_{z_a} - f(v_g - \overline{v})h \\ h \frac{d\overline{v}}{dt} &= (\overline{w'v'})_{z_c} - (\overline{w'v'})_{z_a} + f(u_g - \overline{u})h \end{aligned} \tag{1.9}$$

where the assumption of an incompressible fluid, and with the mean geostrophic wind $V_g = \{v_g, u_g\}$: the last term on the right has the components, with the mean horizontal pressure gradients defined, $u_g = -\frac{1}{\rho_o f} dp/dy$, $v_g = \frac{1}{\rho_o f} dp/dx$.

Finally we require an equation for the rate of growth and decay of the boundary layer thickness. Many methods, simple to complex, are used to describe the growth and decay of ABL thickness. Our purpose here is to show the major components of the budget, rather than to make predictions, and a particularly compact approach due to Smeda (1979), and adopted by Margulis and Entekhabi (2001) suffices. A detailed discussion is found in Garrett (1992) and Stull (1989). Margulis and Entekhabi (2001) assumed that turbulent convection within the mixed layer, the turbulent energy generation by wind, and dissipation are in balance, and, under these simplifying assumptions, they write the Smeda equation in the form:

$$\frac{dh}{dt} = \frac{2\bar{\theta} G_* e^{-\kappa h}}{g h \Delta\theta} + \alpha \frac{\overline{w_s'\theta_s'}}{\Delta\theta} \tag{1.10}$$

where the first term on the right represents the net generation of turbulent energy from forced convection, and the second term represents the net generation of free convection. The quantity G_* is the turbulent energy generation by wind, κ is a turbulent dissipation length scale (Kim and Entekhabi, 1998), and α is a coefficient representing the proportionality in heat flux between top and bottom of the boundary layer. Neglecting the net wind generation term and setting the virtual sensible heat flux of the layer to $H = \overline{w_s'\theta_s'}/\rho c_p$, (1.10) takes the form:

$$\frac{dh}{dt} = \alpha \frac{H}{\rho c_p \Delta\theta} \tag{1.11}$$

which is a simpler approximation that holds when turbulence generation is dominated by buoyant convection from a warm surface. Under these circumstances, buoyancy is provided in proportion to the sensible-heat fluxes from the surface. Under these common, daytime conditions, the growth of the ABL thickness due to convective turbulence that bubbles up from the heated surface, breaching the temperature inversion that caps the ABL, and entraining air from the free-atmosphere above, is roughly proportional (Stull, 1991) to the upward sensible-heat flux from the surface and the inverse of the "strength" of the temperature inversion between the ABL and the (warmer) free-atmosphere above. The coefficient $\alpha \sim 0.2$, according to Stull (1991).

The well-mixed *ABL* will entrain free atmosphere air and grow until a temperature inversion forms that this of sufficient strength to nearly match the turbulence welling up from below, or until conditions at the top of the *ABL* are cool enough so that vapor in air at the top of the ABL begins to condense, at the lifting condensation level (*LCL*). Once the *LCL* is reached, shallow clouds begin to form or cumulus convection can be initiated (if free-atmospheric instabilities allow). The surface-driven convective growth of the *ABL* typically is stalled or overridden by these other processes at this height (Betts, ??). Thus the *LCL* is typically an approximate maximum height that the *ABL* layer can obtain at a given time (although as the thermodynamic state of the *ABL* continues to evolve, the LCL itself may continue to change). At night, or when the surface is cooler than the *ABL*, the *ABL* typically becomes stabilized so that turbulent mixing in much of its daytime domain all but ceases (e.g., Yamada 1979). Under these circumstances, mixing is mostly limited to a relatively thin surface-hugging layer, 10's of meters thick, where turbulence is produced by roughness and shear in the winds at the surface.

Thus, from the simplified equations above, and the preceding discussion of limits of their applicability, we see that, above the canopy, key observations to tie the *ABL* to the underlying layers of the control volume will be *ABL* thickness, mixed potential temperature and mixing ratio, and the inversion jumps of temperature and mixing ratio. With observations of these properties of the *ABL*, the atmospheric heat and moisture "deficits" that—in part—determine rates of latent and sensible heat from the canopy layer can be tracked and predicted. Observations of clouds and/or radiation in the canopy or at the surface must be added to these *ABL* observations to allow the various ABL feedbacks on the surface hydrology to be monitored and understood. The well-mixed model for the atmospheric portion of the control volume has the advantage of removing the usual prescribed land-surface-atmosphere boundary conditions, allowing a physically realistic coupling of the land surface with the atmosphere without a full numerical model of the atmosphere. By integration over the depth of the boundary layer, the forcing requirements are simplified to: incoming solar radiation, large-scale winds, and estimates of large-scale temperature and humidity profiles above the mixed layer.

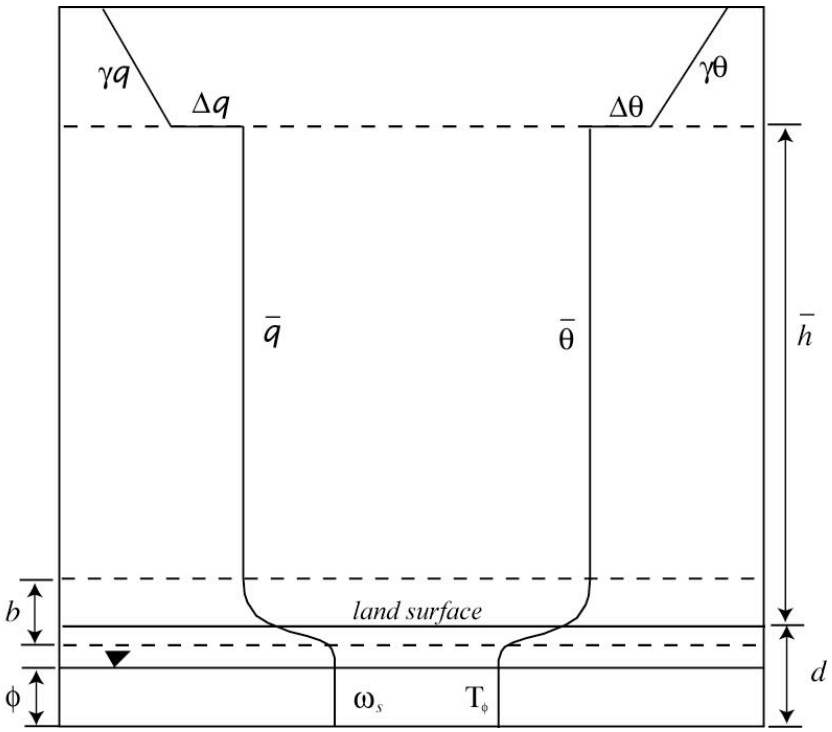

Figure.4 The simplified atmospheric mixed layer distribution for $\bar{q}$ and $\bar{\theta}$. *The subsurface distribution of soil moisture* ω *and temperature* T *are also indicated.*

The Regolith Control Volume

Before proceeding to developing the balance equations, clarification of the active flow depth in the subsurface is required to define a control volume. A working definition of the atmospheric boundary layer or *ABL* (e.g. Garrett, 1989) is the fluid layer directly above the Earth's surface within which the effects of the earth surface are felt directly (friction, heating, cooling), and for which significant fluxes of momentum, heat and mass are transported over relatively short time scales by turbulent exchange. By analogy, we might consider a complementary subsurface volume, defined by our watershed area and some "effective depth" which also feels the direct influence of the overlying surface fluxes and energy fluxes, and which operates at time scales significant to the water cycle and climate within the watershed domain. We suggest that, like the *ABL*, the depth of a

subsurface boundary layer (*SBL*) should be a function of the forcing from the boundaries of the layer (land-surface-atmosphere above, and deep exchange from below). In addition, we require that as the forcing to the subsurface boundary layer relaxes, the layer itself should dissipate. Here we briefly develop a simple argument for why the regolith (or some part of it) serves as a useful way to define an *SBL*, and to quantify the depth of active subsurface flow operating within a watershed.

The physical domain near the earth's surface is referred to as the regolith, and is variously defined (J. B. Field, Advances in Regolith) as the entire unconsolidated, fractured, or secondarily altered surface layer that overlies more coherent bedrock, that has been formed by weathering, tectonics, erosion and/or deposition. It includes soil, biota (from microbes to tree roots), glacial deposits, colluvium, alluvium, aeolian sediments, soil moisture, and groundwater. There are at a minimum, three processes effecting fluid circulation in the regolith:

***Topoclimatic Forcing*:** As observed by Toth (1963), Maxey (1960) and many others, the regional water table (or free surface) tends to be correlated with topography forming a subdued image of the overlying terrain, and intersecting the terrain at major river valleys and stream channels. In the geophysics literature this is sometimes referred to as topographic drive. However, it is clearly the result of the partitioning of water and energy balances at the land surface, including orographic effects.

***Regolith Anisotropy*:** The hydraulic conductivity of the regolith generally has a preferential direction, with typical values of the ratio of horizontal to vertical conductivity in the range: $1 \le K_x^o / K_z^o \le 10^4$, where $K_{x,z}^0$ is the directional hydraulic conductivity. Anisotropy in granular, sedimentary materials is the result of fine-scale

stratified material of varying conductivity, with vertical-average *K* considerably smaller than the horizontal average (Freeze and Cherry, 1979).

***Regolith Heterogenity*:** In addition to topography and anisotropy the regolith exhibits a depth-dependence in hydraulic conductivity as a result of physical, biological, and chemical earth processes, such as: freeze-thaw, rain splash, lithostatic compaction, bioturbation (roots, burrows, etc.), decaying litter from microbial activity, and chemical dissolution/precipitation reactions. Collectively, these processes tend to introduce a depth dependent hydraulic conductivity $K(z)$. With these three processes, a simple model for saturated subsurface flow in our conceptual watershed will serve to demonstrate the concept of the *SBL*. Consider a vertical cross-section of our watershed, where the subsurface flow is simplified to two-dimensional, vertical (x,z) flow is governed by the Laplace equation ($\nabla \bullet (K(z)\nabla h)_{x,z} = 0$), and where $h(x,z)$ is the potential or hydraulic head. (Note: a third dimension doesn't alter the idea appreciably). Assume an anisotropic conductivity of the form, $K_x(z) = K_x^o e^{-z/z_o}$; $K_z(z) = K_z^o e^{-z/z_o}$, and the anisotropy ratio $K_x^0(z) / K_z^0 = const$. The parameter z_o is a length scale defining the scale of regolith heterogeneity with depth (see Kumar, 2004 for estimates of z_o). Next we define the forcing to the upper boundary of our model as a periodic perturbation representing the first mode of the topo-climatic forcing, wavelength $\lambda = 2L$. The upper boundary is chosen so as to satisfy lateral no-flux boundary conditions ($\nabla h(x = \pm L) = 0$) and the condition at depth is $h(z \to -\infty) = 0$. A characteristic of the fundamental mode is that recharge (vertical downward flow) occurs in the upland region, and discharge (vertical upward flow) occurs in the lower valley (*x=0*). A simple solution for these boundary conditions is given by:

$$h(x,z) = \Delta h \cos[\frac{2\pi(L-x)}{\lambda}]e^{\beta z} \qquad (1.12)$$

$(0 \le z \le -\infty)$. This solution along with the streamlines is presented in Figure 5. A reasonable measure of the active flow depth $'d'$ is given by the e^{-1} level of the exponential term, which is analytically determined by solving the Laplace equation for each of the three regolith assumption described:

$$d_1 \sim \beta_1^{-1} = \frac{L}{\pi} \qquad \text{topo-climatic forcing}$$

$$d_2 \sim \beta_2^{-1} = \frac{\mathrm{L}}{\pi}\sqrt{\frac{K_z^0}{K_x^0}} \qquad \text{regolith anisotropy}$$

$$d_3 \sim \beta_3^{-1} = \frac{2z_0}{\left(1-(1+4\frac{\pi^2 z_0^2}{L^2}\frac{K_x^0}{K_z^0}\right)^{1/2}} \qquad \text{regolith heterogeneity}$$

Figure 5 illustrates the effective depth of the subsurface boundary layer for each case using typical values for the parameters. Note that even though the depth is assumed to be infinite, the aspect ratio of the active flow zone d/L is reduced by $1/\pi$, 1/10, and $1/25$, for the 3 assumptions, respectively. Our purpose here was to demonstrate a simple theory for "subsurface boundary layer", which we now define as $SBL \approx d$, or that depth which is actively participating with the local atmosphere through the land surface of the watershed domain.

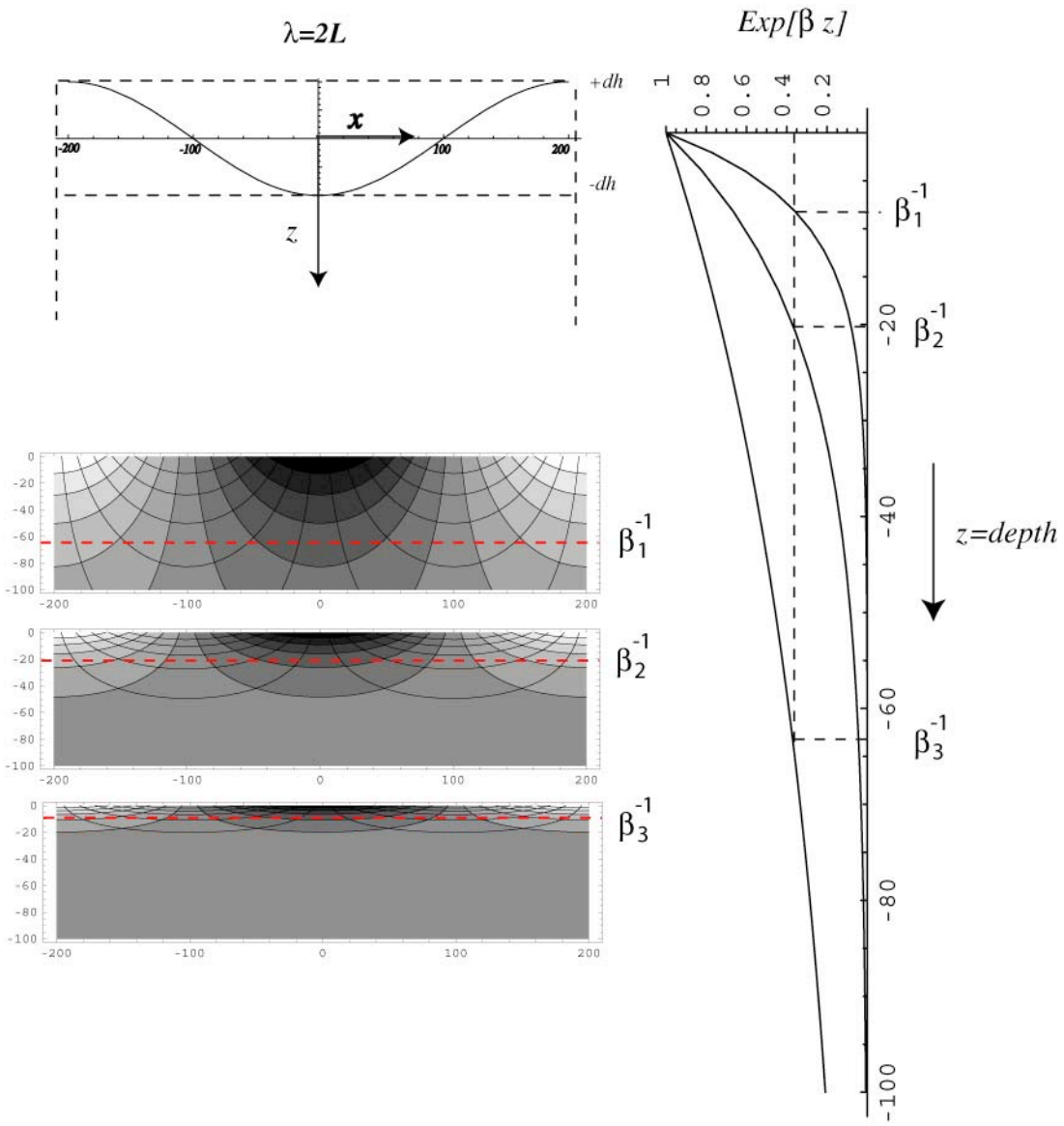

Figure 5. The subsurface boundary layer defined as a depth proportional to the e^{-1} *amplitude attenuation of the shallow water table fluctuation (*$\pm dh$*) for the three cases outlined in the text. The SBL or "effective flow depth" is defined as* $d = \beta^{-1}$ *and note that for values of uniform conductivity (*$K_x^o = 10\ md^{-1}$*), anisotropy (*$K_x^0 / K_z^0 = 10/1$*), and vertical heterogeneity with depth (*z_0 *=10m), the effective depth of active flow is relatively small (<10m).*

Next we develop the balance equations for the regolith control volume, that includes the fully coupled role of soil moisture and water table dynamics (Duffy, 2004).

From the continuity eq. 1.1 and letting our scalar be the soil moisture content (volume water/void volume), $\xi \to \omega$, within the regolith $\mathcal{R}$ as:

$$\frac{\partial \omega}{\partial t} + \nabla \bullet \omega \mathrm{V} + \frac{\partial (w\omega)}{\partial z} = +S_{\omega} \tag{1.13}$$

where once again the divergence terms are separated into vertical (w) and horizontal or plane-flow components ($\mathrm{V} = \{u, v\}$). Also note that time averaging is not carried out in this case, and $F = 0$. Moisture flow within the subsurface layer is complicated by the existence of a free surface boundary or water table (z_o). The layer is partitioned into two parts, where the soil above the water table ($z_o^+ \le z \le z_s$) is governed by gravitational and surface tension forces, with gravity alone below the water table ($z_d \le z \le z_o^-$). The elevation of the free surface is handled as a jump discontinuity, similar to the top of the atmospheric boundary layer. However, the vertical integration of 1.13 will produce two conservation equations which share the jump boundary flux term (Duffy, 1996). Mass conservation for the moisture flux at the moving boundary as we approach the boundary from either side of the interface ($z_o^- \le z \le z_o^+$) is in this case expressed as:

$$\begin{gathered} \omega_{o^+} \frac{\partial z_{o^+}}{\partial t} + (\vec{V}\omega)_{o^+} \bullet \nabla z_{o^+} = \omega_{o^-} \frac{\partial z_{o^-}}{\partial t} + (\vec{V}\omega)_{o^-} \bullet \nabla z_{o^-} = \\ (w\omega)_{o^+} - (w\omega_s)_{o^-} = Q_o \end{gathered} \tag{1.14}$$

where Q_o is the net flux (recharge) to/from (-/+) the water table. Equation 1.14 allows simplification of the vertically-averaged soil moisture and water table of the form:

$$\begin{aligned} \omega_s \frac{\partial \zeta}{\partial t} + \nabla \bullet (\omega \vec{V} \zeta)^+ &= Q_s - Q_o \\ \omega_s \frac{\partial \phi}{\partial t} + \nabla \bullet (\omega \vec{V} \phi)^- &= Q_o - Q_d \end{aligned} \tag{1.15}$$

where ω_s is the moisture content at saturation, ζ is the equivalent depth of soil moisture storage above the water table and ϕ is the depth of saturation below defined by:

$$\zeta = \int_{z_o^+}^{z_s} \frac{\omega}{\omega_s} dz, \quad \phi = \int_{z_d}^{z_o^-} \frac{\omega_s}{\omega_s} dz . \tag{1.16}$$

The flux terms for the soil moisture zone Q_s and Q_o are defined respectively as infiltration/exfiltration through the surface soil layer, and recharge to/from the water table. The flux Q_d admits a vertical exchange with the deeper groundwater layer.

The divergence terms for lateral flow are evaluated by averaging 1.9 over the projected surface area of the control volume (Fig. 3), and by applying the divergence theorem which yields the lateral flow above and below the water table, respectively

$$\begin{aligned} \frac{1}{A}\iint_A \nabla\bullet(\omega\vec{V}\zeta)dA = \frac{1}{A}\int_B (\omega\vec{V}\zeta)\bullet ndB = Q_{\rightarrow}^{+} \\ \frac{1}{A}\iint_A \nabla\bullet(\omega\vec{V}\phi)dA = \frac{1}{A}\int_B (\omega\vec{V}\phi)\bullet ndB = Q_{\rightarrow}^{-} \end{aligned} \tag{1.17}$$

Finally, the balance equations are formed for a fully-coupled unsaturated-saturated flow,

$$\begin{aligned} \omega_s \frac{d\zeta}{dt} = Q_s - Q_o + Q_{\rightarrow}^{+} \\ \omega_s \frac{d\phi}{dt} = Q_o - Q_d - Q_{\rightarrow}^{-} \end{aligned} \tag{1.18}$$

where (ζ,ϕ) are interpreted as volume averages/per unit area. The flux rate Q_s again represents the near-surface flux (infiltration or exfiltration) in units of volumetric flow per unit projected surface area, and $Q_{\rightarrow}^{+}$, $Q_{\rightarrow}^{-}$ define the lateral soil moisture flux and lateral groundwater flow per unit surface area, respectively. From this point we assume that the lateral flow in the unsaturated zone $Q_{\rightarrow}^{+} = 0$ and $Q_{\rightarrow}^{-} \neq 0$. The net vertical flux to/from the water table $Q^0(\xi,\phi)$ represents the integral properties of unsaturated flow and

recharge or evaporation from the water table, as well as the effect of water table motion from lateral groundwater flow. The reader is referred to Duffy (2004) where Q_o, the water table flux, is shown to be a function of both the unsaturated and saturated storage. Figure 7 illustrates the equilibrium relationship between unsaturated storage and saturated storage. Notice that as the water table position ϕ_i increases the available soil moisture storage (e.g. the integral of soil moisture) is actually reduced demonstrating the competitive relation between saturated and unsaturated storage of soil moisture (Duffy 1996, 2004 for detailed discussion). Standard approaches to soil-moisture monitoring and modeling that ingore the effect of saturation implicitly assume the deep water-table limit, so that the water-table/soil-moisture feedbacks are underestimated or neglected. Where and when a zone of saturation develops even temporarily, a very different diurnal evolution occurrs as is also indicated in Fig. 7. In general the water table-soil moisture feedbacks are generally missed by standard approaches. We note that a similar competition is present between the surface turbulent fluxes into the *ABL* and partially contravening fluxes from entrainment of the overlying free atmosphere (equations 1.4). This competition between surface and *ABL* entrainment fluxes is also missed by standard fixed *ABL* approaches (see Margulis and Entekhabi, 2001, for discussion of the "missing" competition).

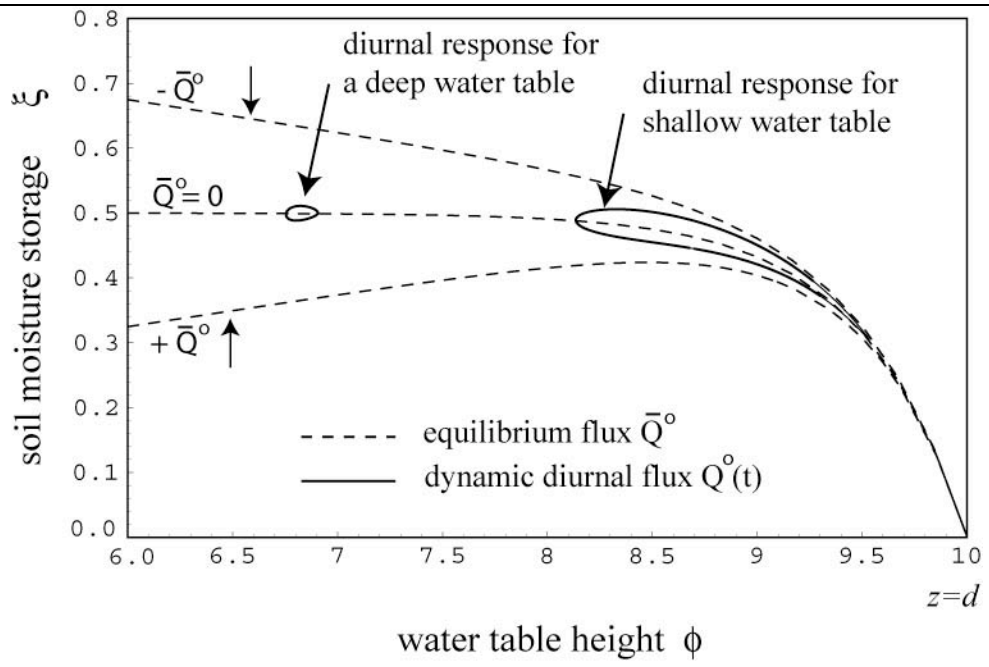

Figure 6. *Phase-plane plot of diurnal response from eq 1.7 to simulate wetting-drying cycles $Q_o(t)$ for deep and shallow water table initial conditions. The regolith depth is 10m of loamy soil. The graph shows the equilibrium effect of infiltration or recharge (-) and exfiltration or evapotranspiration (+) on the water table and soil moisture storage (Duffy, 2004)*

Energy transport within the active flow region follows a similar strategy as before and yields the bulk energy transport equations for unsaturated and saturated storage

$$\begin{aligned} \omega_s c_s \frac{d(T_\zeta \zeta)}{dt} &= c_s T_s Q_s - c_s T_\zeta Q_o \\ \omega_d c_d \frac{d(T_\phi \phi)}{dt} &= c_d T_\zeta Q_0 - c_d T_\phi Q_d - c_d T_\phi Q_{\rightarrow}^{-} \end{aligned} \tag{1.19}$$

where c_s and c_d are the surface and deep soil heat capacity, T_s, T_ζ and T_ϕ are the temperature of the surface soil, unsaturated and saturated zones respectively. Note that we have assumed that the lateral groundwater temperature variation is uniform or the local groundwater temperature is assumed to only change due to vertical mixing (averaging). Expanding the left-hand side of 1.19, substituting 1.18 and simplifying yields

$$\omega_s \zeta \frac{d(T_\zeta)}{dt} = Q_s(T_s - T_\zeta)$$
$$\omega_s \phi \frac{d(T_\phi)}{dt} = Q_o(T_\zeta - T_\phi) \tag{1.20}$$

Note that the shallow or near-surface soil temperature T_g represents a mean for the surface within the transition layer, where seasonal or diurnal changes are the greatest. Also note that the energy flux below the water table is simplified to the vertical temperature difference $(T_\zeta - T_\phi)$ modulated by the vertical flux of moisture Q_o. This assumption allows Q_d and $Q^o_{\rightarrow}$ to be eliminated from the energy balance.

The Transition Control Volume

Thus far we have developed a simple representation for the atmosphere and regolith moisture-energy regimes, and next we develop the moisture dynamics for the transition zone. The above- and below-ground biological component of the control volume is shared with $\mathcal{A}$ and $\mathcal{R}$, with constant thicknesses b^+ and b^- for the canopy and the surface- or root zone layer respectively. Clearly, additional layers can be added to account for spatial structure in soil, vegetation, rooting depth, etc., the present system demonstrates the process equations sufficiently for the objectives of this paper. The specific humidity, moisture content and energy equations for the transition layer $\mathcal{T}$ can be written:

$$
\begin{aligned}
b^{+}\frac{dq_c}{dt} &= P_c - \frac{1}{\rho_o}E_c - Q_{rc} \\
\omega_s\frac{d\zeta_s}{dt} &= P_g - \frac{1}{\rho_o}E_g - Q_s - Q_{rs} \\
c_c\frac{dT_c}{dt} &= R_{nc\uparrow} - H_c - L_vE_c - kc_c(T_c - T_s) \\
c_s\frac{dT_s}{dt} &= R_{ng\uparrow} - H_g - L_vE_g - kc_s(T_s - T_\zeta)
\end{aligned}
\qquad (1.21)
$$

The specific humidity in the canopy (q_c), the equivalent depth of moisture in the surface layer (ζ_s) along with the temperature for each layer are defined as:

$$
\begin{aligned}
q_c &= \frac{1}{b^{+}}\int_{z_g}^{z_{b^{+}}} q dz, \quad b^{+} = z_{b^{+}} - z_g \\
\zeta_s &= \int_{z_{b^{-}}}^{z_g} q dz, \quad b^{-} = z_g - z_{b^{-}} \\
T_c &= \frac{1}{b^{+}}\int_{z_g}^{z_{b^{+}}} T dz, \quad T_s = \frac{1}{b^{-}}\int_{z_{b^{-}}}^{z_g} T dz
\end{aligned}
\qquad (1.22)
$$

The flux term E_c represents the net evaporation plus transpiration from the canopy, Q_s is the net exchange between the surface layer and the unsaturated layer below, E_g represents the net evaporation plus transpiration from the surface layer including low vegetation, and P_c, P_g are the respective precipitation terms. The flux terms Q_{rc} and Q_{rs} represent the root uptake fluxes for the canopy and the surface layers, respectively.

The relationship among moisture fluxes is demonstrated in Figure 7. The important idea is that coordinated measurements are necessary to resolve the moisture (energy) fluxes of this system and that feedbacks at each level are coupled to the adjacent level in a physically plausible way.

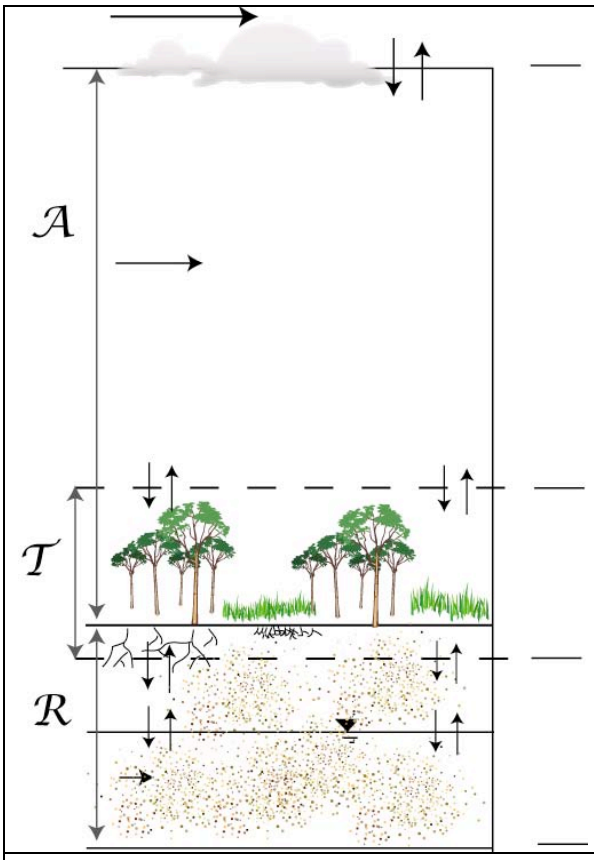

$$E_h = (E_c + E_g) - \rho_0 h \frac{d\overline{q}}{\partial t}$$

(*note: the equations for* $\dot{\theta}, \dot{T}, \dot{h}, \dot{u}, \dot{v}$ *are implied here as well*)

$$E_c = \left(P_c - Q_{rc} - b^{+} \frac{dq_c}{dt} \right) \rho_0$$

$$E_g = \left(P_g - Q_s - Q_{rs} - \frac{d\zeta_s}{dt} \right) \rho_0$$

$$Q_s = Q_o + \omega_s \frac{d\zeta}{dt}$$

$$Q_o = Q_{\rightarrow}^{-} + \omega_s \frac{d\phi}{dt}$$

Figure.7 Water cycle flux estimation equations for each level in the column $\mathcal{A}$-$\mathcal{T}$-$\mathcal{R}$*: entrainment (*E_h*), evaporation and transpiration flux (*$E_c + E_g$*), surface soil flux (*Q_s*), and flux at the water table (*Q_o*). In general the terms on the right hand side would be observed and/or parameterized from observed variables and the system solved simultaneously to estimate the fluxes at each level (left).*

The transition layer can also include cold season processes, and this is accomplished by substitution of moisture (snow and frost) and energy equations within the upper and lower transition layers, respectively. For brevity, we do not include them in the conceptual and mathematical model, but instrumentation is included for integration of the water and energy balance for cold-season processes in a later section.

Coordinated Instrumentation, Data, and Models

Basic Platform Design

Recall that the goal of this paper is to estimate all the important fluxes in a vertical column from "bedrock to boundary layer" and then to regionalize the fluxes over the domain of the watershed. The development and implementation is supported by simplified balance equations formed by integration over the projected volumes forming a dynamical system of coupled equations for the control volume. Taken together, we propose a sensor system that will allow estimation of the important boundary or interfacial fluxes within this framework. In this way the model serves as both a conceptual tool that explicitly defines the particular interface for which the instrument should measure the flux, and as a constraint on the overall energy/moisture budget itself. Next we discuss a particular suite of sensors that can in principal measure all relevant vertical states and/or fluxes at a point in the system.

It is important to recall that the focus of this research is not on instrumentation per say, but rather the coherent measurement of hydrologic fluxes within a prismatic control volume within the watershed domain. Given the wide range of instrument choices available today and specific needs of this experiment, we propose 5 criteria to guide instrument selection: 1) Instruments should be chosen such that each state and/or interface flux assumed in the local model can be measured. 2) Any selected instrument or sensor should be able to support continuous or nearly continuous and unattended operation. 3) The instrument(s) should be able to operate in all weather conditions. 4) Given the need for multiple sensor arrays across the watershed, any instrument selected should be relatively low cost, and not require extraordinary investment in operation and

maintenance. 5) The instrument or sensor selected for deployment should be field-tested and have a record of reliability and accuracy for the state or flux measurement intended.

The basic instrument configuration is illustrated in Figure 8, and includes a "whole canopy" micrometeorological tower configuration, boundary-layer profilers, as well as surface, soil and groundwater observations.

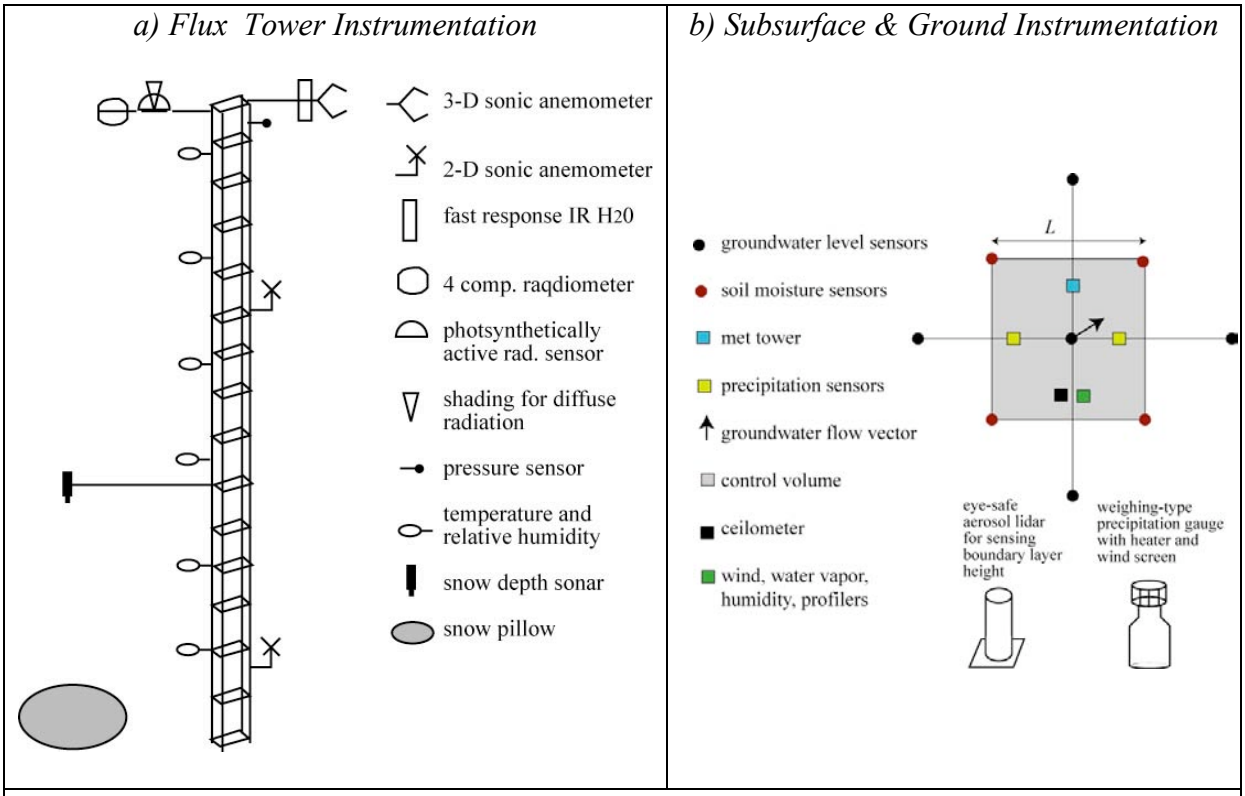

Figure 8: (a) Illustrates the proposed sensor configuration for a micrometeorological tower (25-30 m), (b) the soil moisture array (4 sites and 3-4 depths at each), the groundwater level finite difference array (5 piezometers), redundant precipitation gauges, and a central data collection/transmission site. The piezometers array spacing is deployed to capture the local hydraulic gradient in order to resolve the subsurface advective flow. For example if $\nabla\phi \sim 10^{-3}$ *then L~10m to resolve .01m changes in water level. See text for other descriptions.*

Instrumentation for the basic met tower of Figure 8 follows the well-developed and tested recommendations of the AmeriFlux network (Davis, et al, 2003; Berger et al, 2001). Fluxes of water vapor, momentum, and sensible heat are measured continuously

via eddy covariance, and radiation sensors (hemispheric upwards and downwards solar and terrestrial components, in addition to segregation of direct and diffuse incoming solar and photosynthetically active incoming solar) will provide radiative forcing data from the canopy layer. The eddy-covariance method measures the turbulent transport of a scalar, such as water vapor. This method has been deployed on more than 200 towers across the globe (Baldocchi et al 2001) to collect continuous, long-term measurements of energy, water, momentum and carbon dioxide fluxes Berger et al, 2001; Davis etal, 2003. The tower may also measure CO_2 fluxes and mixing ratios for ecological and carbon cycle research. Many of the processes responsible for hydrologic fluxes are also critical to CO_2 exchange, thus the study of both fluxes often benefits regional budget estimates and model evaluation and development (Baker et al, 2003; MacKay et al, 2002; Helliker et al, 2004).

A ground-based precipitation sensor system must be able to detect the amount, intensity, distribution, as well as to discriminate the different types and sizes of precipitation. An optical disdrometer co-located with a weighing-type precipitation gauge is proposed here. The disdrometer or laser precipitation monitor should detect drizzle, rain, hail, snow, an ice pellets (e.g. www.thiesclima.com). The precipitation load cell requires a wind shield. Both devices require heating elements in cold-weather applications. In the configuration of Figure 8, two precipitation gauges are deployed at the site for redundancy and to provide an estimate of uncertainty for point measurement. Additionally we include instrumentation for barometric pressure (pressure sensor), snow water content (snow pillow and pressure sensor), and snow depth (sonic sensor). For each

of these instruments we adopt the specifications of the SCAN network (Soil, Climate, Analysis Network) of the US Department of Agriculture (www.wcc.nres.usda.gov).

Above the canopy, the mixing volume requires the *ABL* thickness (which determines the size of the "reservoir" into which canopy-level fluxes mix) along with the temperature, humidity, wind speed and direction. The height of the boundary layer is conveniently observed by a lightweight, portable, eye-safe, aerosol lidar, or ceilometer designed for unattended continuous use (e.g. the CHM 15k, www.jenoptik-los.com). The ceilometer should have a useable range from 50-4000m. This instrument may also provide cloud cover information.

Up-looking boundary-layer profilers for monitoring low-altitude wind, humidity, and temperature are necessary for incorporating ABL processes and feedbacks into the integrated monitoring framework proposed here. Much progress has been made in recent years in developing reliable vertical temperature and humidity profiles from ground-based passive microwave radiometers. The accuracy of the profiling radiometers for temperature, humidity and cloud liquid water have been well tested under a wide range of conditions (Liljgren, 2004), and retrievals compare favorably with radiosonde soundings (Gafford and Hewison, 2003). One of the tested systems is the TP/WVP-3000 by Radiometrics which measures both temperature, humidity, and cloud liquid water in a single instrument, including a correction for operation during rainfall. Terrestrial profiling radiometers are cost effective, and provide the high temporal resolution, with good vertical resolution within the boundary layer. Site calibration is conveniently performed with radiosonde soundings.

Modern boundary-layer wind profilers are high frequency or UHF Doppler radars,

which can operate unattended in all-weather conditions. These radars operate by detecting the drift of turbulent eddies with the mean wind, and provide continuous time measurements directly above the site. Although vertical velocity cannot be measured during rainfall, horizontal wind is maintained. An example of commercially available combined wind and thermodynamic profiler is shown in Fig. 9.

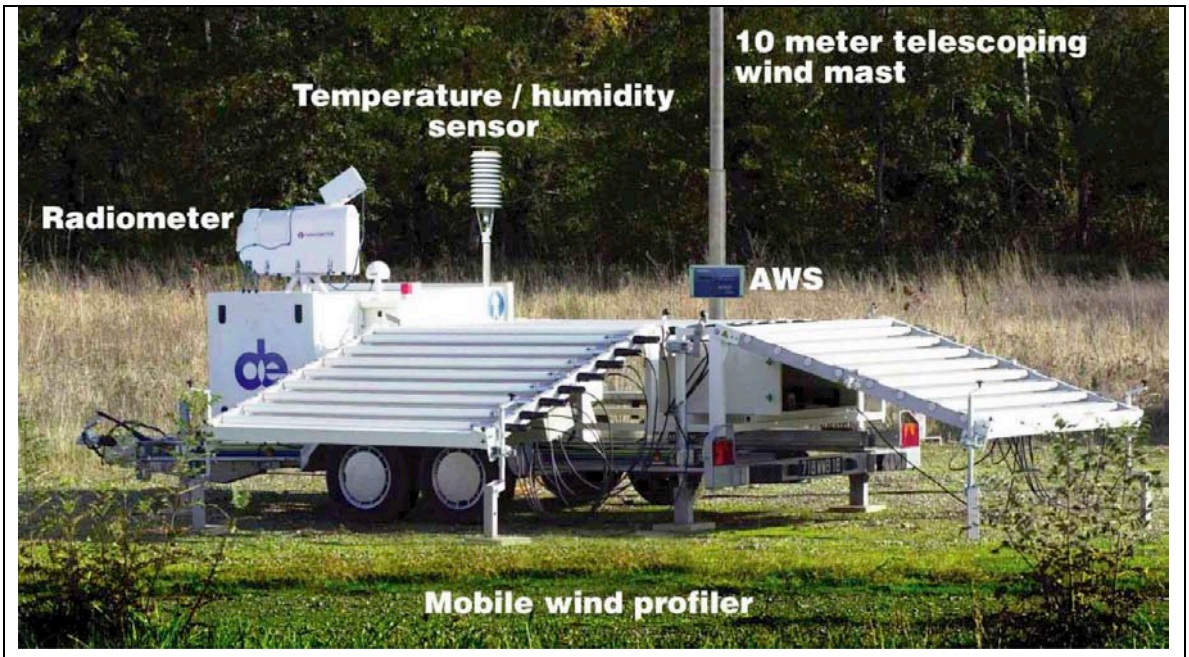

Figure 9. A UHF Doppler wind profiler (PCL1300, www.degreane.com) and microwave temperature and humidity profilers (Radiometric, TP/WVP-3000) for continuous vertical profiling and fully automated, all weather operation.

By projecting the control volume downward to include the soil and shallow groundwater, we propose to include the dynamic changes in the water table as well as the lateral advection of groundwater. Recall that the water table is involved in the following processes: 1) The water table is a lower boundary condition for the soil column, 2) Seasonal water table dynamics and capillary moisture rise above the water table may introduces a source of soil water from below. 3) Under some conditions the waer table may support "hydraulic lift" of water by plants especially during drought periods. 4) The

water table responds to downward infiltration and recharge of snowmelt at the end of the rainy or cold seasons. Experimentally, the piezometer array of Fig. 8 (see Ferris et al, 1962), admits a direct estimation (assuming regolith properties are known) of the flux to/from the water table (e.g. recharge), or lateral flow and translation of groundwater. The latter being the major component of baseflow to streams in the watershed.

Above the water table, paired soil moisture and pressure sensors are deployed. Table 1. illustrates a possible configuration of the subsurface array. The soil pressure head is necessary in the deeper and generally wetter part of the soil profile, where soil moisture becomes insensitive to the flux of water. Note that pressure transducers measure a negative pressure (relative to atmospheric pressure) and a positive pressure below the water table. Piezometers for observing the water table should focus on resolving the flux to the shallow water table. However, it may be useful to add an additional deep piezometer at the center of the array, screened to some depth below the shallow observation point. This will allow the evaluation of deeper upwelling or downwelling flow to/from the array. By coordinating water level sensors below- and soil moisture sensors above the water table, a detailed balance can be achieved using the coupling implied in the model 1.15.

Table. Possible configuration for subsurface moisture, temperature, pressure and/or level array.

Layer	Depth	Moisture	Temperature	Level-pressure
Surface soil	0-5 cm	x	x	x
	15 cm	x	x	x
	30 cm	x	x	x
Deep soil	50 cm	x	x	x
	100 cm	x	x	x
	200cm	x	x	x
Water table	dwt as found		x	x
Deep flow	dwt + 3-5 m		x	x
Note: dwt=depth to water table. The piezometers should be installed 1-3 meter below the water table or deep enough to observe the water level through the annual cycle. The deeper center piezometer should be several meters below the shallow piezometers to evaluate deeper upward/downward flux.				

In the design phase, the precise sensor locations (depth and distance) can be determined by a-priori application of 1.15 with approximate parameters. Thus the model can be used to evaluate soil moisture and water level sensor locations and to assure the correct resolution of the sensors, and the stability of the model equations. In case of a very deep water table (e.g. >15m), or where piezometer drilling is infeasible, the combination of moisture and pressure in the soil profile will allow the flux to be caluculated.Fluxes from all sensors should be computed in real time at the tower and made available online, and raw data will be saved and fluxes computed in post-processing mode for increased long-term accuracy Berger et al, 2001.

Watershed Deployment

The observing platform is meant to begin to resolve the transitions of physical processes at the interfaces within the $\mathcal{A}$-$\mathcal{T}$-$\mathcal{R}$ domain. Figure 10. illustrates how the observing platform could be deployed across the river basin, such that exchanges of moisture across the atmosphere-surface-subsurface system can be observed within the larger network, which scientists have already shown to be strongly scale-dependent (Betts, 2004). Dimensions of course are a design issue as well. The precise positioning and geometry of the local array would depend on the application. Here we assume that the river network is the important design feature and the local arrays are positioned near channels of increasing topological dimension (1^{st} , 2^{nd}, 3^{rd}, etc. order streams).

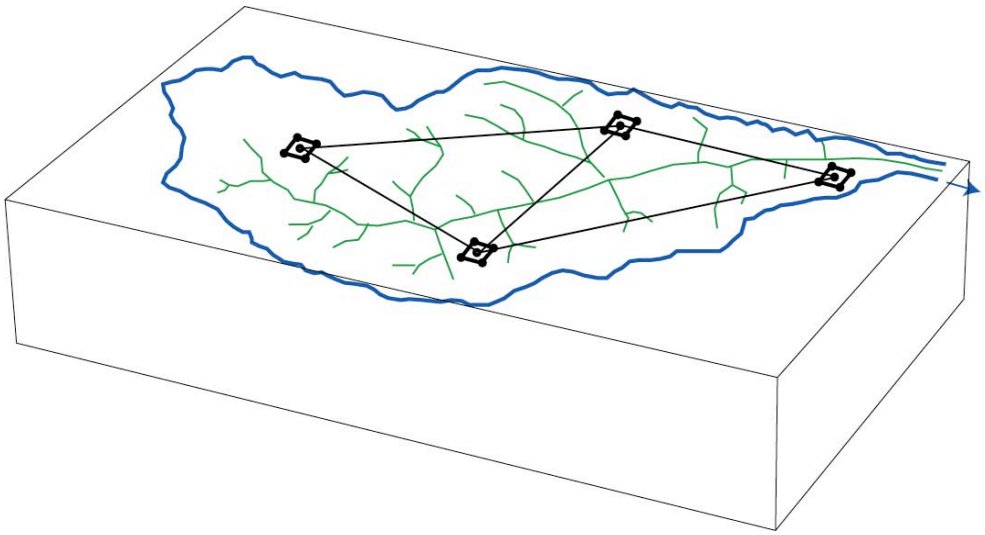

Figure 10. Local observing platform deployed over the river network of the experimental watershed.

The platform would be deployed such that major features of the topography, soils, hydrostratigraphy, and the river network can all be "observed" as a coherent whole. Other information layers such as regional geology, climatic gradients, the coastal-marine interface, and ecological gradients might also be the basis for design.

The particular deployment strategy should also recognize spatial and temporal variability in the exchange of water with the atmosphere from the land surface and canopy represent critical links in the regional-scale water cycle (Avissar 1995). Without a deeper understanding of these processes and fluxes, our ability to conceptualize and mathematically describe them, our predictive models are severely limited. Understanding the influence of heterogeneity in surface vegeation, soil moisture, plant canopy-atmosphere interaction, and the role of preferential flow and recharge to the water table will be greatly improved as a result of the coherent observations. Next we examine how the ground-based network described above is linked to subgrid watershed variability as well as regional instrumentation and models.

Regional Measurements and Models

Up-looking atmospheric profilers and ground-based instrumentation are complementary to scanning instruments from land and space. The strength of the ground-based instrumentation proposed above is the high temporal resolution, while scanning and satellite instruments can provide important spatial structure as well as time information across the watershed. Each type of information is important for prediction and assimilation in forecast models. Here we discuss the collateral instrumentation and models in the experiment.

Clouds and precipitation represent a major forcing of terrestrial hydrologic processes. We expect the experiment should have access to weather radars such as NEXRAD, and meteorological satellites such as CloudSat. Paired precipitation gauges and optical disdrometers deployed over the watershed, can serve to validate these instruments, but the raw information can be most helpful in estimating the spatial distribution of precipitation within the watershed. Improvement in subgrid-scale precipitation, remains one of the most important hurdles to a new generation of the watershed and river basin modeling. Other instrumentation might be to collect information on the three-dimensional air motions of clouds and droplet size using strategically deployed Doppler and other radar systems. These will also provide useful information about air motions and particle physics of non-precipitating clouds that can be used to quantify three-dimensional water vapor structure, cloud structure, water phase, hydrometer advection, and wind fields. Precipitation radars such those of the DOE Atmospheric Radiation Measurement program (Fig. 11) will be crucial for improving weather, climate, and hydrologic models.

Figure 11. State-of-the-art precipitation radar and other instruments at the DOE ARM site.

A promising research area for this effort is the GRACE satellite, a joint USA-Germany mission, with the mission to quantify changes in regional water resources (reservoirs and ground water). GRACE observations together with advanced gravity anomaly models provides for a new powerful tool to track groundwater dynamics and how it will influence climate, weather and water resource availability In the past, regional or large-scale measurement of water in large, inaccessible river basins have been difficult to acquire, while underground aquifers and deep ocean currents have been nearly impossible to measure. Observations of regional mass variations of water at the river basin scale coordinated with a continuous-time network of piezometers will lead to a more powerful indicator of annual to decadal climate change. Similarly changes in

regional ground water will provide critical observational "closure" constraints to hydrological models used for water resources management.

The integration of sensors and systems at the watershed scale is ultimately focused on improvement of predictability and predictive skill where atmosphere-land surface forcing and feedback processes affect extreme events such as drought over intra-seasonal to interannual and decadal time scales. At present we do not have the ability to measure or predict basic characteristics of North American hydroclimatic regimes. The role of dynamic vegetation or the seasonal dynamics of orographic precipitation and snowmelt in mountain are important examples. New data systems, model physics, parameterizations, uncertainty representation, and assimilation tools will be necessary to build the next generation of hydrologic forecasting tools. As one example, the Weather Research and Forecasting (WRF) modeling project is a community effort intended to develop a next-generation mesoscale forecast model and data-assimilation system that will advance both the understanding and prediction of mesoscale weather, and accelerate the transfer of research advances into operations (http://wrf-model.org). The WRF model is state- of-the-art, transportable, and efficient in a massively parallel computing environment WRF offers a range of physics options, on scales down to 1 kilometer and lower resolution for nested subdomains. This makes it an attractive alternative for watershed numerical experiments.

Implications for Climate Research

At present there is no observing platform that integrates instrumentation in the way we have described above. Nonetheless, recent experiments, field campaigns, and

new technologies have largely address the critical issues, and it is useful to briefly explore examples which demonstrate the scientific feasibility and implications of the system proposed here. Hydrologic states with long memory have the effect of integrating past atmospheric forcing, and thus hold the potential to provide useful prediction skill for regional climate modeling. We offer a few examples and challenges where integrated observations are likely to be important to climate research.

Continuous Observations of the Diurnal Boundary Layer Height

The boundary layer height, serves as a fundamental measure of the state of the atmosphere interacting with the terrestrial water and energy cycles, and is a major component of the experiment proposed here. Many authors have shown experimentally and theoretically that land-surface water and energy budgets are strongly coupled to the mixed atmospheric layer above the surface. In particular it is essential that the instrument platform proposed here be capable of observing the diurnal response continuously with all other sensors. Recently, the latest generation of lidar instruments provides portable, eye-safe, low pulse energy, systems that are of relatively low-cost. Figure 12 shows results of continuous *ABL* measurements for one such portable lidar system. This system was successfully applied to study the structure, dynamics, and the evolution of *ABL* using aerosols as atmospheric tracers. Kumar (2006) states that internal sublayers of the *ABL* may also be identified. This result shows the feasibility of using such a lidar system application for continuous *ABL* measurements. Low-altitude wind and temperature profilers for continuous observations are also available using SODAR, passive

microwave, and GPS technologies. (some more discussion here about feedback processes)

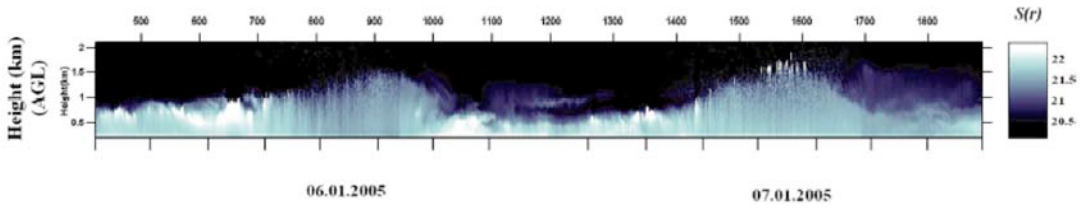

Figure. 12 ABL height evolution for a 2 day period, determined from a portable lidar system that was designed to study the structure, dynamics, and the evolution of ABL using aerosols as an atmospheric tracer (Kumar, 2006). (permission requested)

Vegetation and Feedback in the Transition Layer

The crucial control that vegetation has on the water cycle through its interaction and feedback with the atmosphere and watershed hydrology, requires that we begin to resolve the feedback of vegetation on water and energy fluxes as part of any integrated observing plan. Figure 13 provides a unique example of the coupled atmosphere-vegetation-subsurface system for daily to seasonal time scale from a site in the Rio Grande Valley, New Mexico (courtesy of James Cleverly, UNM). This semi-arid riparian site has cottonwood vegetation, a loamy-sand soil, with a shallow water table. An Eddy Flux tower and observation well array is installed at the site and operated by University of New Mexico scientists (ref.). Although the relationships are complex, the evapotranspiration at the site is strongly dependent on atmospheric conditions and depth to water table. Note that the precipitation at the site is ~20 cm/yr, while the annual evapotranspiration exceeds 1 m/yr. Clearly the water table is an important element of ET in riparian regions.

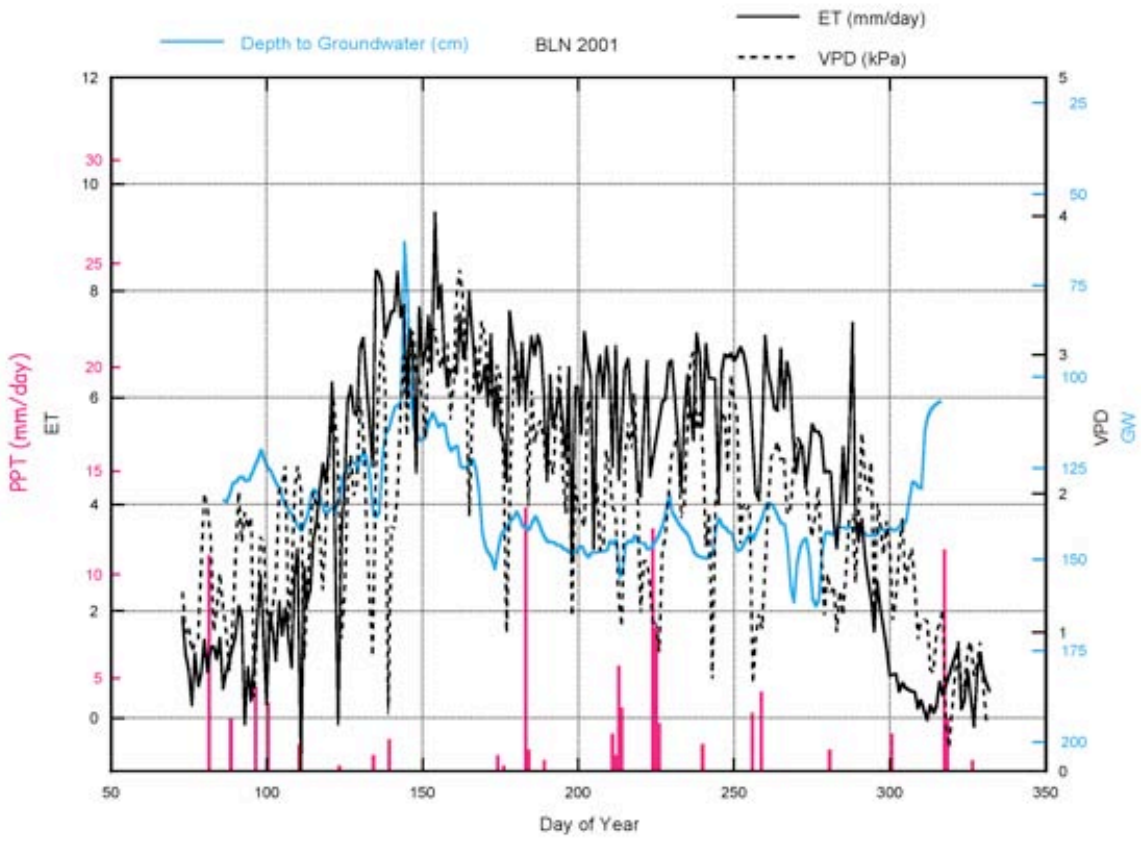

Figure 13. Example of Eddy-Flux estimated ET over a shallow water table from 2001 at Belen, New Mexico. Courtesy of James Cleverly, UNM. The depth to water table is responding to ET and to local effects of river stage within the Rio Grande riparian corridor. The riparian vegetation is cottonwood and salt cedar.

Soil Moisture-Water Table Feedback

Within the regolith, an important feedback process captured in the experimental design proposed here, is the notion of "enslaving" of the soil moisture by the water table as the water table approaches the land surface (Duffy, 2004). The concept was called the Wieringermeer effect by Gilham (1984). Physically, as the level of saturation or water table approaches the land surface, the response of the water table to accretion is amplified since the capillary zone above the water table requires less moisture to saturate. The feedback is an amplification of the water table response during infiltration and the

opposite effect during exfiltration (ET). The concept is observed from an array of shallow observation wells installed on the margin of the Pilot Valley Playa by Donohue, (1984), and illustrated in Figure 14. Note that when the water table is high and near the land surface (elev. ~42.5), the response to recharge events is amplified. As the water table relaxes the diurnal amplitude and the recharge response is reduced. Although the fraction of the watershed subject to shallow water table is limited, it seems reasonable to expect that this effect could temporarily influence the dynamics of saturation and drying of surface soils during after precipitation events as a transient process where the permanent water table is deep. The implications of this effect on net flux of evaporation, transpiration, and recharge are not fully resolved, but could be evaluated with the proposed platform.

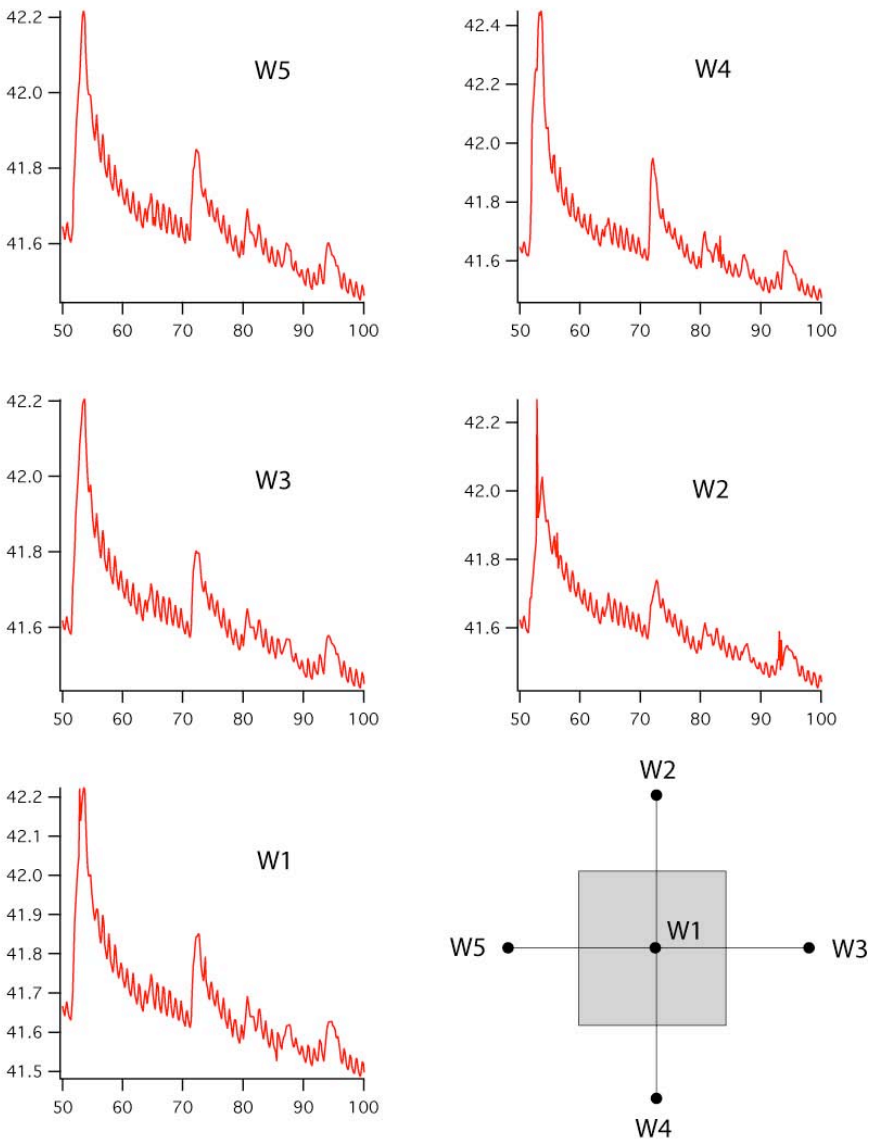

Figure 14. Four hourly water table fluctuations on the margin of Pilot Valley Playa for the period from day 8/21/86 to day 10/11/86, after Donohue (1988). The spacing of the observation wells is 10m, and the elevation of the land surface is ~4200+42.5 m asl.

Summary and Conclusions

The observing platform described here introduces a new level of sensor integration for water cycle research, where the full-canopy met station and Eddy flux is augmented with an arrays of piezometers, soil moisture/pressure/temperature sensors to

estimate vertical and horizontal flux at the plot scale (10-100 m). Wind and thermodynamic profilers and a ceilometer lidar, provide the boundary layer information. Simultaneous measurements will aid in minimizing the "errors" of each subsystem and potentially allow independent, accurate estimates of transpiration, evaporation, and recharge. The array illustrated above, will attempt to provide data sets which close water, energy and mass balances at the plot scale. Additionally, the flux array can potentially (1) serve as a ground validation site for remote sensing studies, (2) help establish new multi-process constitutive relations, (3) useful for assessing the fluid flow and transport in carbon or other water quality studies and (4) aid in elucidating how uncertainty will impact observations and predictions of hydrologic states across multiple-scales. In any given deployment, it is assumed that different sensors and instrumentation from that proposed or inferred here may be necessary. Nonetheless, a strategy based on this general approach, holds the potential to making serious contributions to the problems of energy/moisture feedback for coupling land surface-atmosphere interaction, separation of transpiration form evaporation, measured watershed recharge, antecedent moisture state on feedback on flood and drought behavior.

References (not complete)

Denmead, O. T., M. Raupach, F. Dunin, H. Cleugh, and R. Leuning, (1996), Boundary Layer Budgets for Regional Estimates of Scalar Fluxes, Global Change Biology, 2, 255-264.

Ek, M. B. and A.A. M. Holtslag (2004), Influence of soil moisture on boundary layer cloud development. Journal of Hydrometeorology, 5(10, 86-99.

Gaffard, G. and T. Hewison, 2003, Radiometrics MP3000 microwave radiometer trial report, Tech. Report-TR-26, Met Office, Workingham, UK. 27 p.

Liljegren, J.S., S. Boukabera. 2004. K. Cady-Periera, and S. Clough. The effect of half-width of the 22-GHz Water Vapor Line in retrievals of temperature and water vapor profiles with a twelve-channel microwave radiometer. IEEE Trans. Geosci. Remote Sensing.

Margulis,S. A. and D. Entekhabbi (2001), Feedback between land surface energy balance and atmospheric boundary layer diagnosed through a model and its adjoint, Journal of Hydrometeorology, 2(6), 599-620.

Tennekes, H.(1973), A model for the dynamics of the inversion layer above a convective boundary layer, Jour. of Atmospheric Sciences, 10, 558-567.

Smeda, M. S., (1979), A bulk model for the atmospheric planetary boundary layer. Boundary Layer Meteorology, 17, 411-427.

Randall, D., Q. Shao, C. Moeng, 1992, A second-order bulk boundary-layer model, Jour. of Atmospheric Sciences, 49(20), 1903-1923.

Duffy, C.J., A two-state integral-balance model for soil moisture and groundwater dynamics in complex terrain. Water Resources Research, 1996. 32(8): p. 2421-2434

Duffy, C.J., A Distributed-Dynamical Model for Mountain-Front Recharge & Water Balance Estimation: The Rio Grande of Southern Colorado and New Mexico, in AGU Monograph: Recharge in Semi-Arid Regions: State of the Art, H.a. Scanlon, Editor. 2004.

Ferris, J.G., D.B. Knowles, R.H. Brown, and R.W. Stallman, Theory of Aquifer Tests. 1962, United States Geological Survey (USGS): Washington, D.C. p. 75-77

Gilliam, R. 1984, …

Gordon, J.D., Evaluation of Candidate Rain Gages for Upgrading Precipitation Measurement Tools for the National Atmospheric Deposition Program. 2003, United State Geological Survey: Denver, Colorado. p. 37

Fassnacht, S.R., K.A. Dressler, and R.C. Bales, Snow water equivalent interpolation for the Colorado River Basin from snow telemetry (SNOTEL) data. Water Resources Research, 2003. 39(8): p. 1208, doi:10.1029/2002WR001512

Denmead, O.T., R. Leuning, M.R. Raupach, F.X. Dunin, and H.A. Cleugh, Boundary layer budgets for regional estimates of scalar fluxes. Global Change Biology, 1996. 2: p. 255-264

Yi, C., K.J. Davis, P.S. Bakwin, B.W. Berger, and L.C. Marr, The influence of advection on measurements of the net ecosystem-atmosphere exchange of CO2 observed from a very tall tower. Journal of Geophysical Research, 2000. 105: p. 9991-9999

Wang, W., Regional estimates of net ecosystem-atmosphere exchange of carbon dioxide over a heterogeneous ecosystem. 2005, The Pennsylvania State University: University Park

Baldocchi, D.D., E. Falge, L. Gu, R. Olson, D. Hollinger, S. Running, P. Anthoni, C. Bernhofer, K.J. Davis, J. Fuentes, A. Goldstein, G. Katul, B. Law, X. Lee, Y. Malhi, T. Meyers, J. Munger, W. Oechel, K. Pilegaard, R. Schmid, R. Valentini, S. Verma, T. Vesala, K. Wilson, and S. Wofsy, FLUXNET: A new tool to study the temporal and spatial variability of ecosystem-scale carbon dioxide, water vapor, and enery flux densities. Bulletin of American Meteorological Society, 2001. 82: p. 2415-2435

Berger, B.W., K.J. Davis, P.S. Bakwin, C. Yi, and C. Zhao, Long-term carbon dioxide fluxes from a very tall tower in a northern forest: Flux measurement methodology. Journal of Atmospheric and Oceanic Technology, 2001. 18: p. 529-542

Davis, K.J., P.S. Bakwin, B.W. Berger, C. Yi, C. Zhao, R.M. Teclaw, and J.G. Isebrands, The annual cycle of CO2 and H2O exchange over a northern mixed forest as observed from a very tall tower. Global Change Biology, 2003. 9: p. 1278-1293

Horst, T.W. and J.C. Weil, Footprint estimation for scalar flux measurements in the atmospheric surface layer. Boundary-Layer Meteorology, 1992. 59: p. 279-296

Baker, I., A.S. Denning, N. Hanan, L. Prihodko, M. Uliasz, P.L. Vidale, K.J. Davis, and P.S. Bakwin, Simulated and Observed Fluxes of Sensible and Latent Heat and CO2 at the WLEF-TV Tower using SiB2.5. Global Change Biology, 2003. 9: p. 1262-1277

MacKay, D.S., D.E. Ahl, B.E. Ewers, S.T. Gower, S.N. Burrows, S. Samanta, and K.J. Davis, Effects of aggregated classifications of forest composition on estimates of evapotranspiration in a northern Wisconsin forest. Global Change Biology, 2002. 8: p. 1253-1266

Helliker, B.R., J.A. Berry, P.S. Bakwin, A.K. Betts, K.J. Davis, A.S. Denning, J.R. Ehleringer, J.B. Miller, M.P. Butler, and D.M. Ricciuto, Regional-scale measurements of CO2 flux ans isotope discrimination across the planetary boundary layer. Journal of Geophysical Research, 2004. 109(D20): p. 1-13

Brutsaert, W., Evaporation into the atmosphere: theory, history, and applications. 1982, New York, NY: Reidel.

Kumar, Y. B., 2006, Optical Engineering 45 7 , Portable lidar system for atmospheric boundary layer measurements, 076201 5p.

Lee, I.Y., R.L. Coulter, H.M. Park, and J.H. Oh, Numerical simulation of nocturnal drainage flow properties in a rugged canyon. Boundary-Layer Meteorology, 1995. 72: p. 305-321

Lee, X. and X. Hu, Forest-air fluxes of carbon, water, and energy over non-flat terrain. Boundary-Layer Meteorology, 2002. 103: p. 277-301

Suarez, M.J., Arakawa, A., and Randall, DA, 1983, The parameterization of the planetary boundary layer in the UCLA general circulation model—Formulation and results: Monthly Weather Review, 111, 2224-2243.

Stull, R.B., 1991, An introduction to boundary layer meteorology, Kluwer Academic Publishers, 666 p.

Betts, A.K., 2000, Idealized model for equilibrium boundary layer over land: J. Hydrometeorology, 1, 507-523.

Yamada, T., 1979, Prediction of the nocturnal surface inversion height: J. Applied Meteorology, 36, 526-531.

Huntington, T.G., Glenn A. Hodgkins, Barry D. Keim and Robert W. Dudley, 2004: Changes in the Proportion of Precipitation Occurring as Snow in New England (1949-2000). J. Climate, 17(13), 2626-2636.

Hodgkins, G.A., and Dudley, R.W., 2006, Changes in winter-spring streamflows in eastern North America, 1913-2002: Geophys. Res. Letters, 33, doi:10.1029/2005GL025593.

Stewart, I., Cayan, D., and Dettinger, M., 2005, Changes towards earlier streamflow timing across western North America: Journal of Climate, 18, 1136-1155.

Mote, P.W., A.F. Hamlet, M.P. Clark, D.P. Lettenmaier, 2005: Declining Mountain Snowpack in Western North America. Bull. Amer. Meteor. Soc., 86, 1-39.

Knowles, N., Dettinger, M., and Cayan, D., in press, Trends in snowfall versus rainfall for the Western United States: Journal of Climate, 20 p.

On page 21 of my marked up version, in the discussion of LCLs, I left a ref "(Betts,)" unfinished. A more appropriate reference would be

Freedman, J.M., Fitzjarrald, D.R., Moore, K.E., and Sakai, R.K., 2001, Boundary layer clouds and vegetation-atmosphere feedbacks: Journal of Climate, 14, 180-197.

A somewhat more complete set of refs to the role of the LCL as an approximate "lid" on ABL growth would also include

Bunker, A.F., Haurwitz, B., Malkus, J.S., and Stommel, H., 1949, Vertical distribution of temperature and humidity over the Caribbean Sea: Papers in Physical Oceanography and Meteorology, 11, 1-82. Reprint, Collected Works of Henry M. Stommel, N.G. Hoggs and R.X. Huang, Eds., Vol. 3, Amer. Met. Soc., 1996, 310-368.

Fitzjarrald, D.R., and Moore, K.E., 1994, Growing season boundary layer climate and surface exchanges in a subarctic lichen woodland: J. Geophys. Res, 99, 1899-1917.

Craven, J.P., Jewell, R.E., and Brooks, H.E., 2002, Comparison between observed convective cloud-base heights and lifting condensation level for two different lifted parcels: Weather and forecasting, 17, 885-890.

Yi, C., Davis, K.J., Berger, B.W., and Bakwin, P.S., 2001, Long-term observations of the dynamics of the continental planetary boundary layer: Journal of Atmospheric Sciences, 58, 1288-1299.

Porter, J. N., Lienert, B. R., Sharma, S. K., Hubble, H. W. , 2002, A Small Portable Mie–Rayleigh Lidar System to Measure Aerosol Optical and Spatial Properties , Journal of Atmospheric and Oceanic Technology Volume: 19 Issue: 11 Pages: 1873-1877